CROATICA CHEMICA ACTA CCACAA **69** (1) 125–175 (1996)

ISSN-0011-1643
CCA–2294

Author's Review

Theories of Colloid Chemistry Based on the Point Charge Double Layer Model

Mirko Mirnik

Laboratory of Physical Chemistry, Faculty of Science, University of Zagreb, 10001 Zagreb, P.O.B. 163, Croatia

Received February 9, 1994; revised April 29, 1995; accepted September 15, 1995

In the introduction, the most important colloidal systems and processes which serve for development and checking of the theories of the field, are stressed. On the basis of experimental and theoretical considerations, coagulation is proved to be a process of second order by which small aggregates of up to six singlets are formed. It is graphically demonstrated that the theoretical functions match the experimental ones in an impressive way. The shortcomings of the classical Smoluchowski's (1916) theory are described and proofs are given that the same theory is not a theory of second order reactions, as it should be, and that it cannot be used for explaining of coagulation of big aggregates.

By electron micrographs and by a scheme, it is demonstrated that coagulation in the AgI colloid system consists of three consecutive processes. First, a stable sol containing stable particles is produced by mixing [NaI] and [$AgNO_3$] solutions in appropriate concentrations. After addition of a coagulator to the stable sol, small stable AgI particles in Brownian motion collide and coalesce and primary particles or singlets are formed. The singlets coagulate and form aggregates consisting of increasing numbers of singlets. The space between the singlets in aggregates is filled with intermicellar liquid. The experimental time evolution of the intensity of scattered light is the sum of the decreasing intensity of stable particles function and the increasing intensity of the aggregates function. The square root of the intensity of light scattered, or absorbed, on stable particles or aggregates is proportional to the size of the stable particles or to the number of singlets in the aggregates. Four methods for determination of the half-life or half-period of coagulation from scattered light intensities are described. The theory is supported by experiments of AgI coagulation with two concentrations of [KNO_3], published by Novicki, W., Novicka, G., in *J. Chem. Educ.* **68** (1991) 523–525.

It is suggested that the experimental colloidal crystals are a realization of the quasi crystal lattice which is considered a complementary or alternative Debye-Hückel theory of ionic interactions in electrolyte solutions.
Three types of published plots of molar quotient »$[I^-_{ads}]/[AgI]$ *versus* pAg« are described: the linear plots of freshly precipitated AgI, the exponential adsorption isotherms of coagulated AgI and the curved plots measured on aged and dried AgI. Theoretical functions are proposed for the explanation of experimental plots. A set of measured plots on aged AgI at various concentrations of $0.0001 \leq [KNO_3]$ /mol $dm^{-3} \leq 1.0$ of Figure 5, p. 188 in H. H. Bijsterbosh, J. Lyklema, *Advances in Colloid Interface Sci.* **9** (1978) 147–251. is analyzed on the basis of the same functions. It is demonstrated that the amounts of peptized and coagulated AgI depend on the concentrations of $[KNO_3]$ and on pAg of the solutions in which the aged samples have been immersed. Constants of the theoretical functions are obtained by fitting the theoretical functions to experimental plots. The process of coalescence of peptized small stable particles to form singlets and the coagulation of singlets to form aggregates during »isoelectric« coagulation is explained by a scheme based on published electron micrographs.
Arguments are offered according to which the customary calculation of ζ-potentials, using Smoluchowski's equation from experimental electrokinetic data obtained with colloidal systems is not physically justified.

INTRODUCTION

Motto:

»...though in reality it is a charge consisting of point charges, it is customary to consider it, as first approximation, as a homogeneous surface charge spread over the surface of particles.«

»...and in default of preciser data, we shall, in the following considerations, generally assume the surface charge to be homogeneous.« Overbeek[25]

In the last 50–80 years, many inorganic and organic systems have served for experimental studies of colloidal phenomena. One of the best investigated ones is certainly the AgI system. Different latices are another group of systems that serve the same purpose. The AgI system should serve for elucidation and explanation of the most important colloidal phenomena such as: colloidal stability, coagulation, nucleation, crystallization, recrystallization, aging, heterogeneous exchange, electrokinetic phenomena, *etc.* They all depend on the charges in the double layer and the surface potentials.

The experimental results obtained with the AgI system can be used to develop and confirm theories of stability and coagulation, of double layer structure or surface potentials. They can find many practical applications in sciences, technology, medicine, pharmacy, soil sciences, *etc.* They can be used to explain many processes that occur in natural, industrial and waste waters, like, *e.g.*, separation of precipitates from electrolyte solutions by filtration and sedimentation. Such operations are unavoidable in the production of chemicals, radio-chemicals, dyes, photographic, medical and pharmaceutical materials, in purification of waste waters, in analytical and preparative chemistry, *etc.* Many processes in natural, industrial and waste waters depend on the state of dispersed colloidal substances and their reactions.

It is certain that AgI is one of the best investigated experimental systems that can be used for demonstration and explanation of many of the most important colloidal processes. The investigations were performed in very prominent laboratories.

AgI *Sol Preparation.* If a solution of $AgNO_3$ is mixed with a solution of KI in appropriate concentrations a stable sol is formed. The stable sol consists of small stable AgI particles dispersed in electrolyte. After the mixing of the two precipitation components various processes can be observed. The four most important are: nucleation, stable particle formation and their aging, coalescence and coagulation. The last three processes are illustrated by electron micrographs in Figure 2, while in Figure 3 a schematic explanation is described. The schematic presentation is certainly much closer to reality than the analogous presentations based on the charge density function of homogeneously charged plane surfaces of undefined sizes. As a rule, the present day conventional theories of colloid chemistry are based on the charge density function of homogeneously charged plane surfaces.

Origin of Potentials on Sol Particles. Colloidal particles are always charged and the charges cause electrostatic potentials in their surroundings. The charges are ions adsorbed on the surface of inorganic colloids or ionic radicals chemically bound to the surface of, *e.g.*, latices, macromolecules, surface active substances and other colloidal substances. An equivalent counter charge of ions remains statistically distributed in the electrolyte. The distribution of counter ions is diffuse and it is called »ion cloud«. The charges on the surface together with the counter charge are called »double layer«. The charges on the surface and the ionic cloud are equivalent. The layer between the surface and the bulk of electrolyte is also called »interface« and contains the double layer. It can be considered as a third phase, in addition to the solid and bulk electrolyte phases. There is no reason whatsoever why the interactions of ions forming the double layer in the interface

should not be theoretically treated in the way their interactions in electrolytes are treated. The generally accepted theory of interactions of ions in electrolytes is the Debye-Hückel theory. Its elementary version uses the point charge model for the ions. The best, and correct, model for the ionic double layer is, therefore, the analogous point charge model of the Debye-Hückel theory as applied for the double layer.

The ionic double layer on colloids is incorrectly named »electrical« in the literature. Strictly, electrical double layers exist only on charged polarisable electrodes of Galvanic cells. The models of electrical double layers are those of Helmholz, Stern, Gouy-Chapmann, Grahame and others. They were developed to explain the reactions on polarisable electrodes of galvanic cells. They cannot represent double layers on colloidal particles. Polarized electrodes of Galvanic cells only are charged with electrons originating from an outside battery and the charge of electrons only can be spread homogeneously over metallic surfaces. Charges on metallic stable sol particles are adsorbed ions. No differences in principle in colloidal properties of polarisable metals, *e.g.*, (Au, Pt, Hg), not polarisable metals, *e.g.*, (Ag, Sn, Zn), of ionic solids, *e.g.*, (AgI, $Fe(OH)_3$, Ag_2S), or nonmetals, *e.g.* (S, Se), or different latices were observed. The explanation is in the stabilizing charges that are in all cases either adsorbed ions or chemically bound ionogenic radicals and they cannot be homogeneously spread electrons.

The Nernst potential cannot be formed on the surface of colloidal particles either. It can be measured as the electromotive force between the two poles of electrometers, *i.e.*, between the two ends of the wires connecting the metallic electrodes with the poles of electrometers. The electrodes in the electrolyte can be cowered with a semiconductor, *i.e.*, an ionic solid like AgI, Ag_2S. The Nernst potential on a given electrode does not depend on the electrode itself but also on the reference electrode. It can be positive or negative depending on the reference electrode. Theoretically, it is defined by the difference between the chemical potentials of the oxidized and reduced forms of the potential determining ions, *e.g.*, Ag/Ag^+, Zn/Zn^{2+}, $Ag/AgI/I^-$. The process of charging consists simultaneously of oxidation and reduction of potential determining ions at one electrode and the opposite and equivalent reduction and oxidation at the second electrode. The wires can be connected to the electrodes anywhere, also in a cavity of the electrode. The measured Nernst potential is the electromotive force or the difference of the inner electronic, or Galvanic, or cavity potentials of the indicator and the reference electrode.

The dependence of any hypothetical potential on the logarithm of an ion concentration is, in literature, occasionally called »Nernst«-like. The Nernst potential is defined by the logarithm ion concentration because it is theoretically defined by the chemical potentials. Calling different functions that are theoretically derived from chemical potentials »Nernst-like« is, therefore, not justified and confusing.

Coagulation. One of the purposes of experimenting in coagulation kinetics is the determination of the coagulation rate constant, k_c, which is calculated from the measured time, t, and the experimental half-lives or half-periods, $t_{1/2}$, by $k_c = t/t_{1/2}$.

Coagulation can be induced by addition of coagulators to stable sols. Coagulators can be counter ions of different charge number and many charged or uncharged surface active substances. Counter ions are ions of opposite sign to the sign of ions adsorbed or chemically bound to the surface. Three types of coagulation processes can be distinguished.

The first type of coagulation is that of formation of small aggregates. The second order reaction theory of coagulation, which explains the formation of small aggregates containing up to three primary particles or singlets is published in Ref. 1. and it is supported by the results of coagulation of hard polystyrene and soft polyvinyl latices published in reference.[2] Primary particles or singlets are present in the system before the addition of the coagulator and during coagulation they form, not changing their size or shape, growing aggregates. Stable particles of latices are produced by chemical synthesis. In the present paper the theory of formation of small aggregates is extended to the formation of aggregates containing 4 to 6 singlets and the theory is compared with Smoluchovski's[3] theory of coagulation kinetics which, is critically analyzed.

The second type of coagulation processes are those of the formation of big aggregates[4] consisting of hundreds of singlets. It will be demonstrated that the second order reaction theory can be also used to explain the formation of big aggregates and the theory is supported by coagulation experiments with AgI sols observed by light scattering techniques.[5] No proposal of another theory of coagulation of big aggregates is known to the author.

The third type of coagulation is the »isoelectric« coagulation which can be induced, *e.g.*, by addition of Ag^+ to negative stable AgI sols to obtain $6.5 > pAg > 4.5$ (See Figures 13, 14).[6] (pAg or pI, correspond to pH or pOH, *i.e.*, they are equal to the negative logarithm of $[Ag^+]$ or $[I^-]$ activity or concentration.) The designation »isoelectric coagulation« is inadequate, incorrect and irrational. It is customary and it has been introduced in the past under the assumption that the same coagulation occurs in the point when $pI = pAg = -\log (K_{AgI})/2 = 8$. It was assumed namely, that in the same point the negative electrokinetic ξ-potential, in fact, the negative electrokinetic mobility, becomes positive. In Ref. 6. it was demonstrated, however, that the same transition and coagulation occur in the broad range $6.5 \rightarrow pAg \rightarrow 4.5$ and not in the point $pI = pAg = -\log (K_{AgI})/2 = 8$. In the same range the adsorbed $[I^-_{ads}]$ is netralized and $[Ag^+_{ads}]$ is formed. It was demonstrated also that the negative activity limit of stability, $pAg_{limit} = 6.5$, is =equal in the three halide systems, AgCl, AgBr, AgI, althrough, their ionic products are different.[38]

COAGULATION THEORY OF SMALL AGGREGATES

Coagulation as a Second Order Collision Reaction. During coagulation, the aggregate number sizes, i, can be calculated as long as free singlets are present in a sufficiently high concentration, by

$$1 + i = (1 + i) \tag{1}$$

where $i = 1$ is the number size of a singlet charged with a given number of point charges, usually one, and $i \geq 1$ are number sizes of colliding aggregates. Collision is efficient if, after the collision, new aggregates of number sizes $2 \leq (1 + i)$ are formed. At the beginning of coagulation, $(1 + i) = 2$ and $(1 + i) = 3$ only are formed and later, gradually, also $(1 + i) = 4, 5, 6, \ldots i_{max}$ (Figure 1). In sufficiently long time periods the concentration of singlets of $i = 1$ and the collision rate of the biggest aggregates become too small in such a way that no aggregates of $(1 + i) > i_{max} = 6$ can be formed in acceptable times.

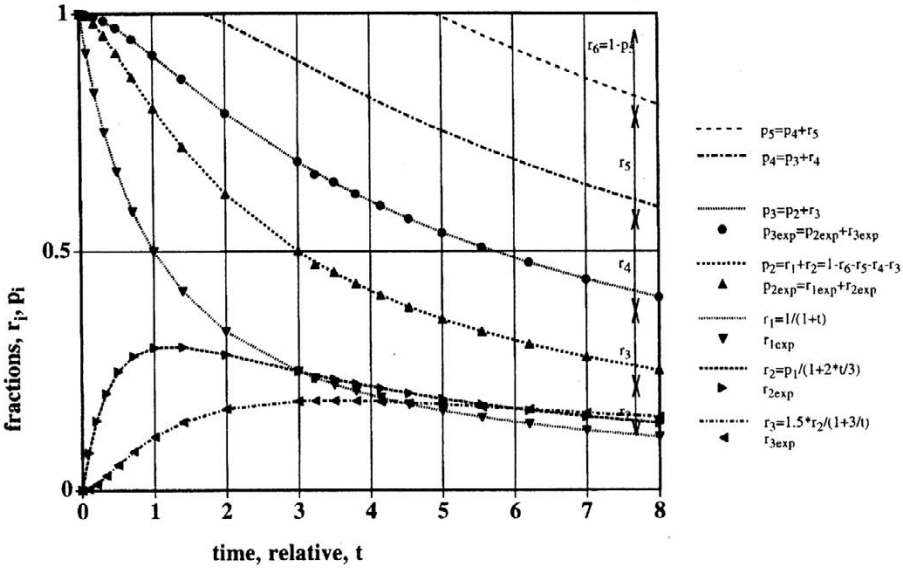

Figure 1. Coagulation of soft polyvinyl latices (Experiments reproduced from 3^2). Ordinate: reactant and product fractions. Abscissa: relative time, t. Lines: theoretical time evolution of number fractions of singlets, r_1, (5); doublets, r_2, (7); triplets, r_3, (8) and their sums $p_2 = r_1 + r_2$, $p_3 = r_1 + r_2 + r_3$. They fit the experimental points of singlet, r_{1exp}; doublet, r_{2exp}; triplet, r_{3exp}, $p_{2exp} = r_{1exp} + r_{2exp}$, $p_{3exp} = r_{1exp} + r_{2exp} + r_{3exp}$ fractions of Figure 3^2. Anticipated functions are $p_4 = p_3 + r_4$, $p_5 = p_4 + r_5$, calculated using Eqs. (5), (7), (8) and, also, $p_4 = 1 - p_3$, $p_5 = 1 - p_4$, $p_6 = 1 - p_5$.

The number of free singlets, n_1, in a given minimal volume (See below) is proportional to the reactant concentration or reactant fraction. Then, the reactant fraction, r_1, is defined by

$$[product] \propto r_1 = n_1/n_0 = \nu_1/n_0, \quad \nu_1 = n_1 \ . \tag{2}$$

The concentration of the reaction product is at any time proportional to the product fraction, p_1, and it is defined by

$$[product] \propto \mathrm{p}_1 = 1 - r_1 = (1/n_0) \sum_{i=2}^{i_{max}} n_i = (1/n_0) \sum_{i=2}^{i_{max}} \mathrm{i} \times \nu_i \ . \tag{3}$$

The number of aggregates of size i is ν_i. The number of singlets of $i = 1$ in aggregates of size $i \geq 2$ is $n_i = i \times \nu_i$ and n_0 is the constant number of all singlets present at any time in all aggregates in a characteristic minimal volume. At $t = 0$ they are all free singlets.

The characteristic minimal volume contains, at any t the sum of all singlets in all aggregates of number sizes $i_{min} \leq i \leq i_{max}$.

The elementary second order kinetics equation (See Appendix[A1]), which can be applied to coagulation of singlets, reads

$$t_r = [product] \ / \ [reactant] = (1 - r_1)/r_1 \ . \tag{4}$$

The fraction of the decreasing number of free singlets is proportional to the concentration of reactant, [*reactant*], and can be defined by

$$[reactant] \propto r_1 = 1 - p_1 = 1/(1+t_r) \ . \tag{5}$$

The increase of the concentration of all singlets in all aggregates of $2 \leq i \leq i_{max}$ is proportional to the product concentration, [*product*], and can be defined by

$$[product] \propto p_1 = (1 - r_1) = 1/(1 + 1/t_r) = t_r/(1 + t_r) \ . \tag{6}$$

The relative time of singlet coagulation is $t_r = t/t_{1/2}$. The absolute time is t, and $t_{1/2}$ is the half-life or half-period. At $t_r = 0$ $p_1 = 1 - r_1 = 0$ and at $t_r = 1$, $p_1 = 1 - r_1 = 1/2$, at $t_r \to \infty$ $r_1 \to 0$ and $p_1 \to 1$.

All disappearing free singlets are transformed into aggregates of size $2 \leq i \leq i_{max}$. The fraction of all singlets that are transformed into aggregates of $2 \leq i \leq i_{max}$ is p_1.

The fraction of doublets, r_2, can be calculated as proportional to the increasing number fraction, p_1, divided by $(1 + t_2)$ in analogy to Eq. (7), however, with the relative time $t_2 = (2/3) \times t_r$. This means that the half-life of

doublets is 2/3 of the half-life of the coagulating and disappearing free singlets. The corresponding equation reads

$$r_2 = p_1(1 + t_2) . \tag{7}$$

The proportionality factor (2/3) was obtained by fitting Eq. (7) to experimental values $r_{2\text{exp}}$ and it can be explained by the relative rates of disappearance of doublets of $i = 2$ and of the formation of triplets of $i = 3$.

One can define a function $p_2 = r_1 + r_2$. Function $1 - p_2 = (1/n_0) \sum_{i=3}^{i_{\max}} n_i$ is proportional to the sum of all singlets transformed into aggregates of $i \geq 3$.

The functions of singlet fractions transformed into aggregates of $i \geq 3$ read

$$r_i = (i/2) \times r_2/(1 + 1/t_i) . \tag{8}$$

This was obtained assuming that doublets defined by r_2, Eq. (7), are reactants for aggregates defined by r_i of $3 \leq i \leq i_{\max}$ in relative half-lives $t_i = t_r/i$.

By fitting Eq. (8) for $i = 3$ to $r_{3\text{exp}}$, $t_3 = t_r/3$ has been obtained. Factors 2, 3, i, are obviously caused by the sizes of the aggregates taking part in the formation of aggregates of $3 \leq i$ from doublets of $i = 2$.

The sum of fractions of singlets in aggregates of $3 \leq i$ can be calculated by $p_i = p_{i-1} + r_i \leq 1$. In short periods of coagulation for $i \geq 4$ is the calculated $p_i > 1$, while $p_i \leq 1$ should hold. In the period when the by Eq. (8) calculated $p_i > 1$, r_i must be calculated by $r_i = 1 - p_{i-1}$.

The half-lives for $i \geq 4$ in Eq. (8) must be anticipated and cannot be checked experimentally because no corresponding experiments are known.

The proposed theory satisfies the unavoidable requirement that, at any $0 \leq t_r \leq 9$, for $1 \leq i \leq i_{\max} = 6$, the sum of all singlets in all aggregate fractions should be $p_6 = \sum_{i=1}^{6} r_i = 1$ and $r_7 = 0$. The same condition is a consequence of the mass conservation law. The same periods $0 \leq t_r \leq 9$ are realistic and feasible and most probably aggregates of $i > 5$ start to sediment earlier. Then Eq. (8) does not hold any more quantitatively.

The higher is the i the longer is the t_r necessary to obtain $p_i = 1$. Theoretically, one can consider as the essential period of coagulation the period when $t_r \leq\approx 9$ and $r_1 <\approx 1/10$ of all singlets have remained free and have not been transformed into aggregates. Then $t_r \leq 9$ and $p_i = \sum_{i=2}^{i<=6} r_i \leq 1$ and $r_7 = 0$.

In Figure 1, the discussed functions are plotted and the experimental data from Figure 3^2 are inserted as points for the measured $1 \leq i \leq 3$. In the same way, the remaining experiments of Figures 2 to 6^2 were checked. In all cases the functions of r_1, r_2, r_3 match the experimental points excellently and in this way support the correctness of the second order coagulation theory of small aggregates of $1 \leq i \leq 6$. The r_4, r_5, r_6 and p_4, p_5, p_6 plots were anticipated and could not be checked because the corresponding experiments are not known. It is certainly a very logical supposition that doublets are reactants for the formation of all aggregates of $i \geq 3$ because for $i = 3$ $t_3 = t_r/3$ was obtained by fitting. The anticipated functions r_4, r_5, r_6 in Ref. 1. were erroneous.

One can conclude that the experiments of reference[2] confirm the here proposed application of the second order reactions theory for coagulation of small aggregates.

SMOLUCHOWSKI'S COAGULATION THEORY

Smoluchowski[3] in 1916 published his classical »*Versuch* einer mathematischer Theorie der Koagulationskinetik kolloider Lösungen« or translated »An *attempt* at a mathematical theory of coagulation kinetics of colloidal solutions«, based on, at that time scarce sufficiently exact experimental observations of coagulation kinetics. The charges were erroneously assumed to be homogeneously spread on the surface. Obviously, Smoluchowski himself was not convinced that his proposed theory was correct and final because he called it an »attempt«. Thus far, many papers have been published considering the theory in principle correct but no exact quantitative experimental confirmation of its correctness has ever been provided. Probably, for this reason, modifications and extensions of the theory have been proposed that should be valid for »idealized« systems based on »hypothetical processes« assumed to influence the coagulation rate.[7–9] According to the author's knowledge, up to now, the scientists of the field have not been aware that Smoluchowski's theory can neither explain coagulation of small, and still less, coagulation of big aggregates. Explanation of the same claim follows.

The Smoluchowski's kinetics equation (24)[3] of the »fast« time evolution of aggregate number fractions can be written in the nomenclature of the present paper and in the elementary form[A2]

$$v_i / v_0 = n_i / (i \times n_0) = (t \times \alpha \times v_0)^{-2} \, [1 + 1/(t \times \alpha \times v_0)]^{-(i+1)} \, . \qquad (9)$$

If one sets $\alpha \times v_0 = 1/t_{1/2}$ and $t_r = t/t_{1/2}$, then one obtains

$$v_i / v_0 = (n_i / i) / n_0 = t_r^{-2} [1 + t_r^{-1}]^{-(i+1)}, \; n_0 = v_0 \, . \qquad (10)$$

The sum of all aggregates in a characteristic volume reads

$$S_v = \sum_{i=1}^{\infty} v_i / v_0 = \sum_{i=1}^{\infty} t_r^{-2}(1 + t_r^{-1})^{-(i+1)} . \qquad (11)$$

Here, α is the collision probability erroneously assumed constant and independent of the aggregate size. The number of free singlets in a characteristic volume at $t_r = 0$ is $n_0 = v_0$.

The sum, $S_v = \sum_{i=1}^{\infty} v_i$ (See Figure 13) is, like Eq. (5), a decreasing, *i.e.*, a second order reactant kinetics function. It follows that, according to Eq. (11), in relative times $0 < t_r \to \infty$, the sum of all aggregates of $1 \leq i \to \infty$ represents reactants and that no products exist in the coagulating system. It also follows from Eq. (11) that at $t_r = 1$ $r_1 = v_1/v_0 = 1/4$ while it is a logical requirement that at $t_r = 1$ $r_1 = v_1/v_0 = 1/2$. Function S_v (Eq. (11)) is in principle incorrect because it is the only decreasing function that represents the time evolution of coagulation and at the same time it is the only function that represents the total amount of dispersed colloid present at any time. The total amount of the colloid must be constant. This impossible and erroneous result is a consequence of the impermissible summation of summands, v_i in Eq. (11), which represent different masses, amounts or number sizes of aggregates each.

The assumed collision probability $\alpha \times v_0$ cannot be constant because it must depend on the aggregate mass or size, i. (Pay attention to the isotope effect: the heavier the isotope, the slower are its reactions!). Since at $t_r = 0$ $v_i/v_o = 1$ and $\sum_{i=2}^{\infty} v_i/v_0 = 0$, one must conclude that at $0 < t_r \to \infty$ the sum $\sum_{i=1}^{\infty} v_i/v_0$ is a decreasing, reactant function according to Eq. (5) and that no products are present. Functions (9), (10) are not second order reaction functions like Eq. (5) as they should be if they were caused by second order efficient binary collisions, as assumed by Smoluchowski at the start of his deductions.

In real systems it is, in principle impossible that in a finite volume and at any $0 < t_r$ all aggregates of $1 = i \to \infty$ should be present, even if in infinitesimally small concentrations. Equation (11) cannot be applied to an analysis of real systems. The precision of numerical evaluation of $S_v = \sum_{i=1}^{\infty} v_i/v_0$ depends on the highest i with which the summation is performed or on the computer capacity and not on the characteristics of the coagulating system.

Actually, Smoluchowski's Eqs. (1) to $(24)^3$ correspond by analogy to the present Eqs. (1) to (8), *e.g.*, the present Eq. (5) valid for singlets of $i = 1$ corresponds to Eq. $(24)^{3, A2}$ valid for $S_\nu = \sum_{i=1}^{\infty} \nu_i / \nu_0$.

Besides the already described theoretical arguments, the following additional arguments justify the claim that Smoluchowski's theory cannot be applied to the explanation of coagulation processes in real experimental systems.[1]

(a) The supposed bases of Smoluchowski's theory are binary collisions which must result in a second order reaction mechanism. The resulting original kinetics equations $(24)^3$ of different aggregates are not of the second order, as they should be.

(b) The probability of collisions is not a function of the spherical aggregate radii, as supposed by Smoluchowski. It is a function of the mass concentration (= proportional to the number of singlets in a given volume or to the number sizes of aggregates) as are all processes, physical and chemical. The aggregates of hard latices are not dense spheres; they are sponge like clusters of singlets of very irregular shape. The space betwen singlets in the aggregates is filled with intermycellar liquid. This also means that the aggregates should be defined by their mass, which is proportional to $n_i = i \times \nu_i$ or $\sum n_i = \sum i \times \nu_i$ (See Eqs. (2), (3), rather than by the number of aggregates ν_i or $\sum \nu_i$). The summation of addends of different mass units is physically and mathematically impermissible for real systems. (*E.g.*, $(i = 1) + (i = 2) = n_{i=2} = 3$ is proportional to mass, and the sum $(i = 1) + (i = 2) = \nu_{i=2} = 2$ cannot be used in equations based on the mass.)

(c) The decreasing sum, $S_\nu = \sum \nu_i$ is equal to the second order decreasing kinetics equation (5) and the aggregates of different sizes, i, coagulate by higher order, very improbable, mechanisms each.

(d) The original Smoluchowski's functions[3] of the time evolution of singlets, doublets and triplets cannot be fitted[1] to experimental plots of reference.[2]

The same arguments certainly invalidate also any possible explanation of real coagulation processes by any modified or corrected Smoluchowski's equation.

COAGULATION THEORY OF BIG AGGREGATES

Stable Particles. Electron micrographs in Figure 2, 1.1–1.5, illustrate small colloidally stable AgI particles in the absence of a coagulator and their aging with time. The sol was prepared by mixing NaI with $AgNO_3$ solutions. Such aging is a process of dissolution of the first formed smallest stable particles accompanied by the growth of bigger crystallites. The same process is

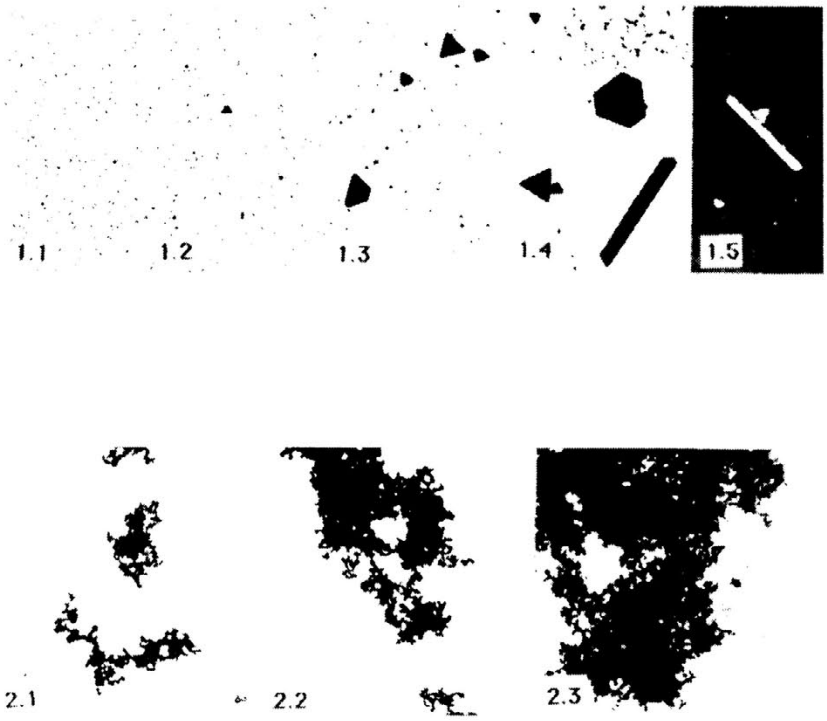

Figure 2. Electron micrographs of a sol [AgI] = [KNO_3] = 2×10^{-4} mol dm^{-3}, pI = 2.5.
Figure 2.1. Small stable AgI particles and their aging: 1.1:10 min., 1.2:100 min., 1.3: 1 day, 1.4: 9 days. Right upper corner: not sedimented stable particles after 17 days. 1.5: after 16 days, vaporized with Pd.
Figure 2.2: Coagulation of singlets to form increasing aggregates. Coagulator: [$La(NO_3)_3$] = 1.0×10^{-4} mol dm^{-3} Singlets in aggregates are bigger than stable particles: 2.1: 1 min., 2.2: 10 min., 2.3: 100 min.

occasionally named »Ostwald's« ripening or aging. Aging or recrystallization occurs in periods of days. Aging should not be understood and interpreted as a process of »slow coagulation«.

If, in the absence of a coagulator, the concentration of iodide, [I^-], or silver ions, [Ag^+], defines pI < 11.5 or pAg > 4.5, the stable sol particles are charged with adsorbed iodide ions, I^-_{ads}. The counter charge is, according to the Debye-Hückel theory, a statistically distributed diffuse »cloud« of cations. The volume density and radial charge density are functions of distance from the reference ion. The maximal radial charge density[A3] function is a sphere of the Debye-Hückel radius,[A4] $r = 1/\kappa$. In collisions caused by Brownian motion, the maximal cation charge counter ion densities overlap,

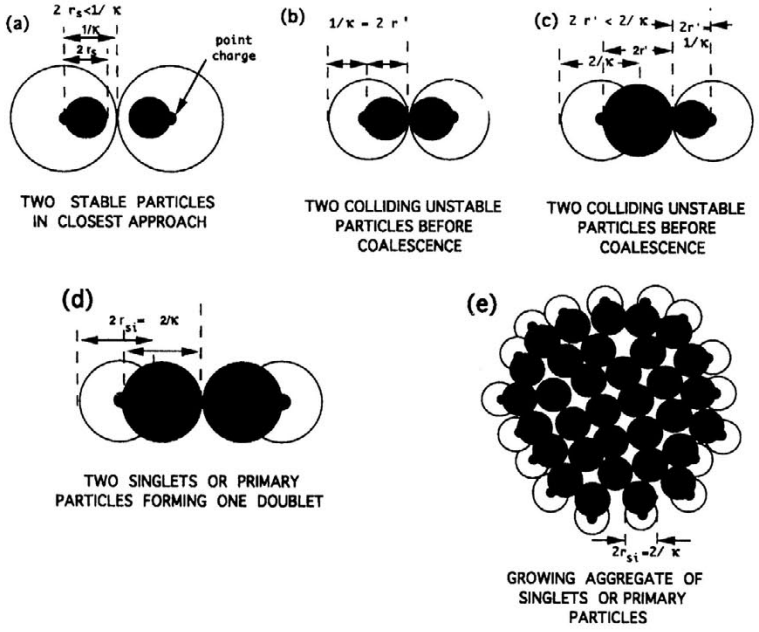

Figure 3. Schematic explanation of coagulation of AgI:
(a) two small stable particles of $2r < 1/\kappa$ in closest approach during an inefficient Brownian motion collision.
(b) Efficient collision induced by addition of a coagulator causing a decrease of $1/k > 2r$ to $1/\kappa = 2r$. The surfaces are in contact and the particles will coalesce due to the van der Waals forces.
(c) Example of one particle of $2r = 1/\kappa$ in collision with another containing 7 particles of $2r = 1/\kappa$
(d) Two singlets of $2r = 1/\kappa$ form one doublet.
(e) By repeated collisions growing aggregates are produced. If $t \rightarrow \infty$, the number of singlets in an average aggregate $n \rightarrow \approx 150$ and the average number of singlets in the radius $n_r \approx 4.8$. The real aggregates are of a very irregular form and many stick together during sedimentation. Note: The possible influence of the dielectric constant of dense particles upon the symmetry of the ionic atmosphere is neglected!

the particles are in closest approach and repel each other before their surfaces come in contact. (See Figure 3a). The collisions are inefficient and the sol is colloidally stable.

Formation of Singlets from Small Stable Particles and their Counter Ion Coagulation. Electron micrographs show that stable particles in Figures 2, 1.1, are small in comparison with singlets constituting aggregates in Figure 2, 2.1–2.3 The latter figure illustrates the growth, with time, of aggregates in the presence of the coagulator La^{3+}. From the same electron micro photo-

graphs the radius of stable particles is estimated to be $r_s < 1/\kappa$ (Figure 3a, schematic) and that of singlets is estimated and taken for theoretical reasons as $r_{si} = 1/\kappa$. Before addition of the coagulator counter ion, the ionic strength, *e.g.* of $I <\approx 1 \times 10^{-3}$ mol dm^{-3}, of the $|z_\pm| = 1$ electrolyte warrants colloidal stability because then $2r_s < 1/\kappa = 9.96$ nm. In Brownian collisions, the electrostatic repelling force between the colliding particles is bigger than any attracting force.

Addition of a coagulator counter ion of $|z_\pm| = 1$ leads to an increase of ionic strength to $I >\approx 10^{-1}$ mol dm^{-3}. The addition of a coagulator counter ion of $|z_\pm| \geq 2$ causes the increase of the electrochemical potential. Coagulator counter ions in sufficiently high concentration cause a decrease of $1/\kappa <\approx 9.96$ nm to $1/\kappa = 0.996$ nm (Figure 3a, 3b). Then small, dense, stable AgI particles of $2 \times r' \geq 1/\kappa$ repeatedly collide efficiently (Figure 3c). Due to repeated collisions, by which the surfaces come in contact, the van der Waals attracting forces are effective in such a way that the particles coalesce and bigger dense particles of $2 \times r' \geq 1/\kappa$ are formed till $2 \times r_{si} = 2/\kappa$ (Figure 3c). At each coalescence, one I^-_{ads} is desorbed because at $2 \times r < 2/\kappa$ the repelling electrostating force between two I^-_{ads} is stronger than the adsorption force. If the diameter of particles becomes $2 \times r_{si} = 2/\kappa$, they do not increase any more and they become primary particles or singlets of the future aggregates (Figure 3d, 3e). The particles of $2 \times r_{si} = 2/\kappa$ are very stable and do not grow further because, after the desorption of one I^-_{ads} on each colliding singlet, the Van der Waals attraction of the surfaces between two singlets causes, instead of coalescence, coagulation, *i.e.*, bigger and bigger aggregates are formed of the increasing number size, i. Now the coalescence would cause that the distance between two charges on one singlet to be $2 \times r_{si} > 2/\kappa$, for which reason the electrostatic repulsion between the two charges on one singlet would be too weak.

According to the Debye-Hückel theory, namely, the equilibrium distance is $2 \times r_{si} = 2/\kappa$. If between two ions $2 \times r_{si} > 2/\kappa$ they attract each other; if $2 \times r_{si} < 2/\kappa$, they repell each other.

The size of the aggregates can be expressed by the number of singlets that they contain, *i.e.*, by their (singlet) number size i (Figure 3d, e). The size is a function of time (See Eqs. (15), (16)). The space between the singlets is filled with the dispersing liquid.

It follows from adsorption measurements by the radioactive tracer technique[10,11] that in the range $3 < \mathrm{pI} < 6$ the molar quotient $\gamma = [I^-_{ads}]/[AgI] = 3 \times [Y^{3+}_{ads}]/[AgI]$ of AgI coagulated with Y3+ is

$$0.0033 < \gamma = [I^-_{ads}]/[AgI] = 3 \times [Y^{3+}_{ads}]/[AgI] < 0.002 \ . \qquad (12)$$

Its reciprocal value, $1/\gamma$, represents the average number of units of AgI to which one I^-_{ads} is adsorbed and equals $303 < n = 1/\gamma < 500$. This means that,

with a decrease of pI, the increase of the singlet size in aggregates is relatively small. The aggregates are of a very irregular form. Assuming that, before sedimentation, aggregates of number size i form spheres of an average number, i_r, of singlets in the radius, then $i_r = \sqrt[3]{3 \times i/(4 \times \pi)} = 0.62 \times \sqrt[3]{i}$ holds. A hypothetical spherical aggregate of average number size, *e.g.*, $i = 113$, has $i_r = 3$ singlets in the radius. Approximately, Figure 3e represents such an idealized aggregate.

The results obtained by the radioactive tracer technique for counter ion adsorption are, within the limits of their precision, equal to those obtained by the potentiometric method obtained for the adsorption of $[I^-_{ads}]$.

In the given concentrations, coagulation occurs in periods of tens or less of minutes. It takes several tens of minutes before the sedimentation of aggregates becomes observable by a fast decrease of the scattered light intensity.

Figures 2 are reproduced from reference[6] where additional information on the processes in AgI sols are illustrated by electron micrographs.

The Second Order Coagulation Theory of Big Aggregates. The number of singlets in an aggregate of number size i is i. The average number of aggregates in the characteristic volume is ν_{av}. After a sufficiently long time in big aggregates hundreds of singlets (Figures 2.2, 3e) are charged with a single I^-_{ads}. The aggregates sediment, the Brownian motion becomes negligible, and their electrophoretic motion cannot be observed. Instead of the electrophoretic motion the electroosmotic transport through membranes can be measured. Membranes can be prepared by sedimentation or centrifugation or filtration of coagulated AgI.

Figure 3 is a schematic explanation of the growth of stable particles till they become singlets and of the coagulation of singlets to form aggregates of an increasing number size.

The possible influence of the presence of solid particles upon $1/\kappa$ and on the symmetry of the ionic cloud in their surroundings is neglected. The same influence is certainly at the present elementary level of discussion insignificant and would not change the principal conclusions. The same applies to Figure 14.

At any time, the number size, i, of aggregates is between the minimal, average and maximal values, *i.e.*, $i_{min} \leq i \leq i_{av} \leq i \leq i_{max}$ The aggregates are of a very irregular form indeed. The space between singlets in the aggregates is filled up with intermicellar liquid. The gradual disappearance of stable particles together with the increase of the number size of aggregates represent coagulation and its kinetics can be observed, among others, by light scattering techniques.[5]

Coagulation is caused by efficient collisions between free singlets and between singlets and aggregates and between aggregates of different i. This

occurs after the addition of a coagulator. Since any aggregate can collide with any other, efficient unit collisions can be described by

$$i'' + (i - 1) = (i'' - 1) + i \ .$$

The smaller the aggregates $(i'' - 1)$ become, the higher is their collision rate, the shorter is their half life and they react faster and faster and, finally, the smallest aggregates disappear. As free singlets of $i = 1$ diffuse from bigger and bigger volumes and collide with the already formed aggregates of $2 \leq i$, first a histogram[4] is formed in very short times compared with $t_{1/2} = 1$. (See Table I, and II).[4] The number size of aggregates in histograms $n_i(j)$, *i.e.*, the number, n_i, of singlets in aggregates of a given number size i, in the characteristic volume, is a function of i_{av} and j.

The progress of coagulation is represented by an increase of all aggregates of $i_{\min} \leq i \leq i_{av} < i \leq i_{\max}$ with time. The histogram must be symmetric, and its number sizes can be characterized by $i_{av} - i_0 + j \leq i_{av} + i_0 + 1 - j$, for $1 \leq j = i \leq i_0$ and the number of singlets in aggregates of size i, at any t, is defined by

$$n_i = i \times \nu_i = j \times 2^j \ . \tag{13}$$

Sizes $i_{\min} = i_{av} - i_0 + 1 \leq i \leq i_{\max} = i_{av} + i_0$ define the width of the histogram. The average aggregate size is defined by $i_{av} = S_0 / \nu_{av}$ and S_0 follows from (14). After the histogram has been formed in a very short time, $t_r << 1$, the coagulation continues by increasing in smallest steps of $\Delta i = 1$ of all $i_{\min} \leq i \leq i_{av} \leq i \leq i_{\max}$.

Base 2 in Eq. (13) is an unavoidable consequence of binary collisions and the second order reaction mechanism. Base 2 is, namely, the smallest possible integer bigger than one. All i and n_i are also integers. For the aggregates of $i \leq i_{av}$ to react, it must be $n_i = 2 \times n_{(i-1)}$ and for the aggregates $i > i_{av}$ to be produced, it must be $n_i = n_{(i-1)}/2$. Aggregates of $i_{av} - i_0 + j$ are reactants for aggregates $i_{av} + i_0 + 1 - j$, which are products of coagulation.

The sum[A5], S_0, of the number of singlets, n_i, in all aggregates of all sizes, $i_{\min} \leq i \leq i_{\max}$, is, at any time, in the same characteristic volume, constant and defined by

$$S_0 = 2i_0 \sum_{j=1}^{i_0} 2^j = 4\, i_0(2^{i_0} - 1) = i_{av} \times \nu_{av} \tag{14}$$

where ν_{av}, is the average number of aggregates of average size i_{av}. For, *e.g.*, $i_0 = 6$ $S_0 = 1512$. The characteristic volume contains at any t_r all aggregates $i_{av} - i_0 + j \leq i_{av} \leq i_{av} + i_0 + 1 - j$ for $1 \leq j \leq i_0$. For a check of coagulation theories the sols must not be monodisperse.

Instead of i_{av}, one can use its fraction, $y_a = i_{av}/S_0$. Both, since proportional, increase with time, t_r, while v_{av} decreases. Proportional to i_{av} is the product concentration, [product], and the product fraction $y_a = i_{av}/S_0$. It holds, namely, that [product] $\propto i_{av} \propto \psi_a = i_{av}/S_0$ and $S_0(y_a) = \sum_{i_{min}}^{i_{max}} y_a = 1$.

Proportional to the reactant concentration, [reactant], are [reactant] $\propto (S_o - i_{av})/S_0 \propto (1 - y_a) = y_r$. The reactant fraction is $y_r = 1 - y_a$.

Since coagulation is a binary collision process, its kinetics equation must be of second order and it can be written in respect of product or aggregate fraction[A1]

$$\frac{i_{av}}{S_0 - i_{av}} = \frac{y_a}{1 - y_a} = \frac{1 - y_r}{y_r} = t_r$$

or

$$y_a = \frac{i_{av}}{S_0} = \frac{t_r}{(1 + t_r)} . \tag{15}$$

Consequently, in respect of the reactant fraction, the following holds

$$y_r = (1 - y_a) = \frac{1}{(1 + t_r)} . \tag{16}$$

Intensity of the Light Scattered by Stable Particles. If a light beam is falling on dense stable particles and aggregates the light is scattered on them. If they are small, as compared with the wave length of the incident beam, the intensity of scattered light obeys exactly the Rayleigh's law.

The basic equation of Rayleigh's theory can be written in the simplified form for the light scattered on small, dense stable particles

$$I_s = B_s \times v_{sav}^2 \tag{17}$$

i.e., the intensity of scattered light is proportional to the second power of the average stable particle volume, v_{sav}, or particle mass, and to their amount concentration. Then, B_s is the proportionality constant valid for the given refraction indexes of dispersed dense stable particles of constant concentration and average volume, v_{sav}, for a given dispersing electrolyte, wavelength and intensity of the incident beam, angle and distance of observation and the scattering volume of the system. This means that B_s is constant for a given system and measuring device provided the

concentration of dense stable particles and their size do not change, *i.e.*, if v_{sav} = cons. If the average number, ν_{av}, decreases and the average volume v_{sav}, increases, B_s is not constant.

Intensity of the Light Scattered by Aggregates. After addition of a coagulator, in the early period of the coagulation process, the volume of stable particles, characterized by its average value, v_{sav}, increases till their average radius, r_{sav}, becomes equal to the Debye-Hückel radius $1/\kappa$,[A4] (See Figure 3), which in turn, is defined by the ionic strength, I.

In the presence of a coagulator counter ion, instead by the ionic strength, I, and the Debye-Hückel radius, $1/\kappa$, r_{sav} is defined by the concentration of the coagulator counter ion and of its charge number z. The counter ions of $z \geq 2$ are present in very low coagulating concentrations and they practically do not change the low ionic strength, I, of the stable sol. The dependence of the molar coagulation concentration, $[M^z]$, on the charge number $\pm z$ is known as the Schulze-Hardy rule of coagulation. Its »linear« formulation reads

$$\ln\left\{|z| \times \frac{[M^z]}{[M^0]}\right\} = -|z| \times S \ . \tag{18}$$

Here, $[M^z]$ is the molar coagulation concentration of the counter ion of charge number $\pm z$, $[M^0]$ is the constant of Eq. (18), which can be obtained by extrapolation of the line to $|z| = 0$ and S is the linear Schulze-Hardy rule proportionality constant. Proportional to the electrostatic energy contribution for coagulation is $-|z| \times S$ and $\ln\{M^0\}$ is proportional to the chemical energy contribution.

The coagulation concentration can be defined, *e.g.*, by a well defined, easily observable coagulation rate. In the past, different investigators used different criteria for the definition of the coagulation rate or coagulation concentration. The coagulation concentration defined by a criterion for the coagulation rate is called critical coagulation concentration, *c.c.c.*

Formulation (18) is predicted by the ion exchange theory of coagulation[12, 16] and has been repeatedly confirmed experimentally[A6] (See Figures 1, 2, 3,[13] 4,[14] 12[25]).

In electrokinetics, in constituent and counter ion adsorption one can define analogous critical concentrations, *c.c.*, which depend on the charge number, z, and they all obey the above formulation[10, 15, 16]. The functions of the cited experimental variables change in *c.c.* drastically.

Particles of diameter $2 \times r = 1/\kappa$ (See Figure 3d) can be called primary particles or singlets. In efficient collisions, they form aggregates and the average number size, i_{av}, of aggregates increases with time (See Figure 3e).

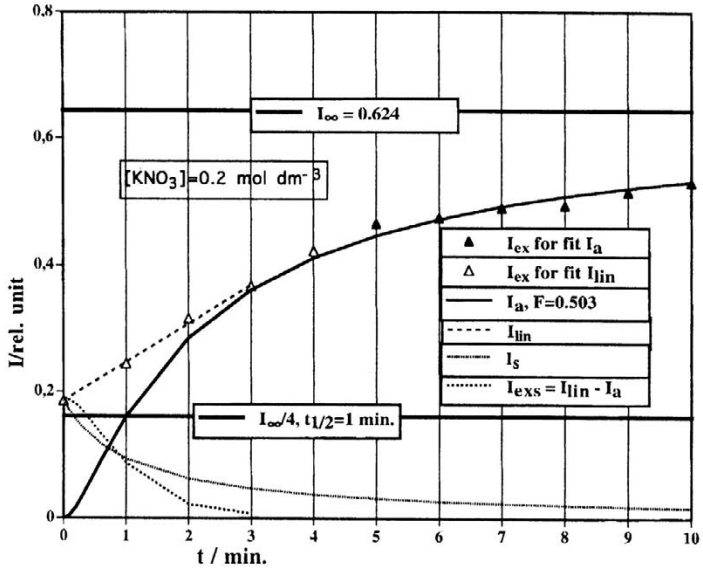

Figure 4. Coagulation kinetics of the sol: [AgI] = 0.04 mol dm^{-3}, [KI] = 0.02 mol dm^{-3}, [KNO_3] = 0.2 mol dm^{-3}. Ordinate: absorbency, *I/rel. unit.* Abscissa: time, t/min. Experimental points from Figure 2[16]: I_{ex}: aggregate formation or coagulation plot (20): I_a, $I_\infty = 0.624$, $F = 0.503$. Experimental stable particle plot: $I_{exs} = I_{lin} - I_a$. Theoretical stable particle plot (25): I_s. The slope of the tangent on I_{ex} for $t \to 0$ cannot serve for determination of $t_{1/2}$!

Intensity of the light scattered on aggregates is proportional to the second power of volume, v_{av}, of average aggregates, or to the second power of their number size, i_{av}.

The basic equation of Rayleigh's theory can be written in a simplified form for the intensity of light, I_a, scattered on aggregates

$$I_a = B_v \times v_{av}^2 = B_i \times i_{av}^2 \ . \tag{19}$$

Here, B_v, B_i are the proportionality constants valid for aggregates defined by their average volume, v_{av}, or by their number sizes, i_{av}. They are constant for a given refraction index of singlets in aggregates plus the intermicellar liquid in the aggregates, all dispersed in a given electrolyte, wavelength and intensity of the incident beam, angle and distance of observation and the scattering volume of the system. This means that B_v, B_{iav} are constant for a given system containing dispersed aggregates in a given measuring device. The constants for stable particles and aggregates are different.

From Eqs. (2) and (3) one obtains

$$y_a^2 = I_{ar} = \frac{I_a}{I_\infty} = \left[\frac{t_r}{(1+t_r)}\right]^2 . \tag{20}$$

The same equation can be transformed into

$$\sqrt{I_{av}} = \frac{\sqrt{I_a}}{\sqrt{I_\infty}} = y_a = \frac{t_r}{(1+t_r)}, \quad I_a \xrightarrow{t_r \to \infty} I_\infty , \quad y_a \xrightarrow{t_r \to \infty} 1 . \tag{21}$$

Values I_0 and I_∞ are, in an ideal case, proportional to B_s and B_i of Eqs. (17), (19). For t_r = 1, $I_a = I_\infty/4$. The present day availability of fitting programs makes it possible to determine $I_a = I_\infty$ and $I_a = I_\infty/4$ directly by fitting Eq. (20) to experimental plots and calculate $t_{1/2}$.

Although equation (20) has been obtained from experimental data, it is ideal and equal for any set of values of F, $t_{1/2}$, I_0, I_∞. All parameters necessary for the definition of any experimental system reduce to the four cited constants.

Light Scattered by Coagulating Sols. In a coagulating sol, in early periods, stable particles and already formed aggregates are present at the same time. The size of the former increases, their number decreases and they finally disappear, *i.e.*, they are all transformed into singlets which are constituents of the aggregates. The number of singlets in aggregates increases with time. Between the singlets in the aggregates is the intermicellar liquid (See electron micrographs 2.1–2.3 in Figure 2.).

If the stable particles and their concentration are sufficiently small, $I_0 << I_\infty$ is small and can be neglected or subtracted as zero effect from the measured I_{ex}. In our laboratory light scattering experiments were usually performed at such low concentrations (See *e.g.*, Figures 1, 2[13]). However, the following exact method should be applied if stable particles are present in significant concentrations.

Experiments suggest that, in the early stages, the total scattered light intensity, $I_{ex}(t)$, is a linear function of t, (See Eqs. (22), (23), Figures 4, 5) and after I_{lin} becomes equal to I_a, the function is defined by Eq. (20) or Eq. (21). Then, all stable particles have coalesced and they have all disappeared because they have all been transformed into singlets and all singlets form increasing sponge-like aggregates.

The measured experimental intensity, I_{ex}, is the sum of the light scattered on dense, growing, stable particles of a decreasing number concentration and on increasing aggregates. Since the volume, v_s, of each stable particle increases their number ν_s decreases and also I_{exs} decreases. Stable particles are transformed into singlets, the latter coagulate and immediately

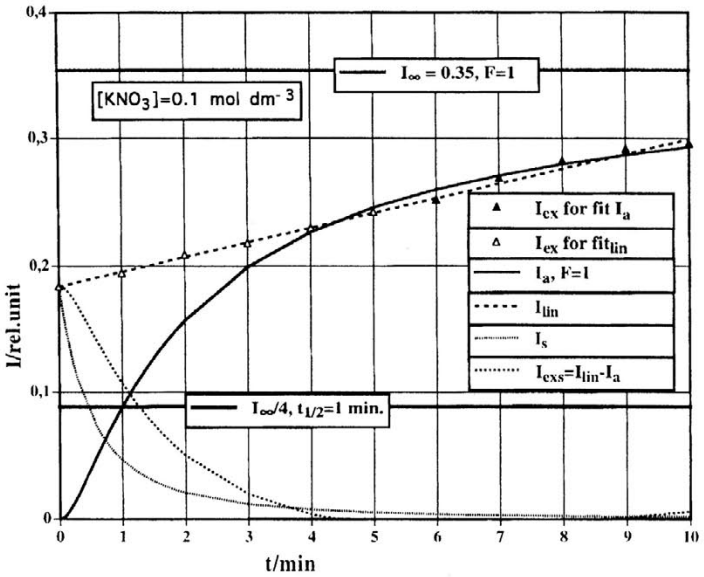

Figure 5. Coagulation kinetics of the sol: [AgI] = 0.04 mol dm^{-3}, [KI] = 0.02 mol dm^{-3}, $[KNO_3]$ = 0.1 mol dm^{-3} : Ordinate: absorbency, *I/rel. unit.* Abscissa: time, *t*/min. Experimental points, I_{ex}, from Figure 2[16]. Aggregate formation or coagulation plot, (20): I_a, I_∞ = 0.354, F = 1. Experimental stable particle plot: $I_{exs} = I_{lin} - I_a$. Theoretical stable particle plot (25): I_s. The slope of the tangent on I_{ex} for $t \to 0$ cannot serve for determination of $t_{1/2}$.

form aggregates. The resulting experimental intensity is defined in the starting period of coagulation by

$$I_{ex} = I_{lin} = I_0 \times (1 + F \times t) \ . \tag{22}$$

It can be transformed into

$$I_{linr} = \frac{I_{lin}}{I_\infty} = \left(\frac{I_0}{I_\infty}\right) \times \left(1 + F \times t_r\right) \ . \tag{23}$$

Analysis of Coagulating Systems Based on the I_s – and I_a – Functions. Usually, only experimental $I_{exr}(t) = I_{ex}(t)/I_\infty$, at relative times $0.01 \approx< t_r <\approx 9$ or at times of $t >\approx 30$ s, can be measured using simple conventional mixing techniques and acceptable precision. At shorter times, in low sol concentrations, the error of measured t is too big due to the relatively long duration of the preparation by mixing the precipitation components of the coagulating sol.

At present, due to the availability of fitting programs, the constants F, I_∞ and $t_{1/2}$ can be obtained by fitting Eq. (23) to the corresponding experimental I_{ex} points. Value I_0 is directly measured at $t = 0$. As a rule, I_∞ cannot be measured directly because, at longer times, the measured values are lower than Rayleigh's theoretical values and because of the possible sedimentation caused by aggregates that have become too big.

Very instructive experiments on coagulation kinetics of AgI sols observed by light absorption[17,18] will be used here to demonstrate an analysis of experiments, as a support to the validity of the second order coagulation kinetics theory and of the usefulness of light scattering measurements and Rayleigh's light scattering theory in experimental coagulation kinetics.

Figures 4 and 5 show the experimental points I_{ex} and the theoretical plots, I_{lin}, I_a, I_s, I_{exs}. The I_{ex} points were taken from Figure 2.[17]

By fitting (20) to points $t_r = 0$ and 3, $4 \leq t_r/\text{min.} \leq 10$, *res.*, the constants I_∞ and $t_{1/2}$ were determined.

By fitting I_{lin} Eq. (22) to I_{ex} for points 0 to 3 or 4 minutes, *res.*, the constant F was determined (See Figure captions).

Evidently, the slope F of I_{lin} neither defines directly the rate of disappearance of stable particles nor the coagulation rate.

The difference

$$I_{exs} = I_{lin} - I_a > 0 \tag{24}$$

represents the real decrease of I_{exs} as it follows from the linear part of the experimental I_{ex} points and from the calculated I_a function with the aid of constant I_∞, which was obtained by fitting.

The theoretical decrease of the light scattered by stable particles, I_s, reads

$$I_s = \frac{I_0}{(1+t)^2} \quad or \quad I_{sr} = \frac{(I_0/I_\infty)}{(1+t_r)^2} \,. \tag{25}$$

Equation (25) would hold if B_s were constant, *i.e.*, if the small, at $t = 0$ present stable particles were singlets that directly coagulate and form aggregates.

It can be transformed into

$$y_s = \sqrt{I_{sr}} = \frac{(\sqrt{I_0}/\sqrt{I_\infty})}{(1+t_r)} \,. \tag{26}$$

All four theoretical functions depend solely on the precision of the determination of the three constants. The precision of the cited constants depends on the number of measured points and on the first and last measured t and, of course, on the instrument and technique used.

The theoretical $y_s = \sqrt{I_{sr}}$ function, Eq. (26), is proportional to the decrease of the number concentration of small stable particles under the assumption that the small stable particles are singlets which immediately and directly coagulate and form aggregates, *i.e.*, that B_s = cons. Since stable particles increase and their number concentration decreases, they cause, together with aggregates, the increasing linear, I_{lin}, part of the I_{ex} plot.

Since in both [KNO_3] concentrations (Figures 4 and 5) for $I_a = I_\infty/4$ is $t = t_{1/2}$ = 1 min., and t_r = 1, it follows that $I_a = I_\infty/4$ defines the half-life, $t_{1/2}$ = 1 min, of coagulation in both cases. Unexpectedly, certainly exceptionally, the absolute, t, and the relative, t_r, scales are equal and one can conclude that the coagulation rate, which is defined by $t_{1/2}$ = 1 min, does not depend on the two cited counter ion concentrations, [KNO_3], I_∞ = 0.643 and 0.354 and F = 0.0611 and 0.0115, *res.* are different. One must conclude that S_0 is smaller and I_{av} bigger in the lower [KNO_3]. (See Eq. (14)). This is in accordance with the claim that the singlet size depends on the Debye-Hückel radius, $1/\kappa$, *i.e.*, on the ionic strength, I, of the coagulator counter ion electrolyte. The rate of transformation of stable particles into singlets is higher in the higher [KNO_3] because F is higher.

The slopes, F = 0.0618 and 0.0115, *res.*, obtained by fitting I_{lin} to the I_{ex} plots for $0 < t <\approx 3$ and 4 min., *res.*, are a proof that the same slopes can neither be used for estimation of $t_{1/2}$ of the coagulation nor can they be used for estimation of $t_{1/2}$ of the disappearance of stable particles.

Analysis of Coagulating Systems Based on the $\sqrt{I_a}$ *and* $\sqrt{I_{ar}}$ *Functions.* One can transform the I_a plots, Eq. (19), into the $y_a = \sqrt{I_{ar}} = \sqrt{I_a}/\sqrt{I_\infty}$, Eq. (21), plots, which are equal for any I_∞ and $t_{1/2}$ value obtained by fitting in various systems and sol concentrations.

Besides the already described method of estimation of $t_{1/2}$ from experimental I_{ex} plots in Figures 4 and 5, the following three methods can be proposed based on the theoretical $y_a = \sqrt{I_{ar}} = \sqrt{I_a}/\sqrt{I_\infty}$ plots, Eq. (21), and described by Figures 6, 7, 8.

Figure 6. presents the experimental points $\sqrt{I_{exr}} = \sqrt{I_{ex}}/\sqrt{I_\infty}$ and theoretical functions $y_a = \sqrt{I_{ar}} = \sqrt{I_a}/\sqrt{I_\infty}$, (21), $\sqrt{I_{linr}}$, (23), $\sqrt{I_{exr}}$, Eq. (24), $\sqrt{I_{sr}}$, Eq. (26), obtained for [KNO_3] = 0.1 mol dm^{-3} are drawn.

The main advantage in comparison with Figure 5, is the equality of the square root of scattered light intensity and of number fraction plots, *i.e.*, $y_a = \sqrt{I_{ar}} = \sqrt{I_a}/\sqrt{I_\infty}$. As a consequence, t_r = 1 if $y_a = \sqrt{I_{ar}} = 1/2$, in accordance with the definition of $t_{1/2}$.

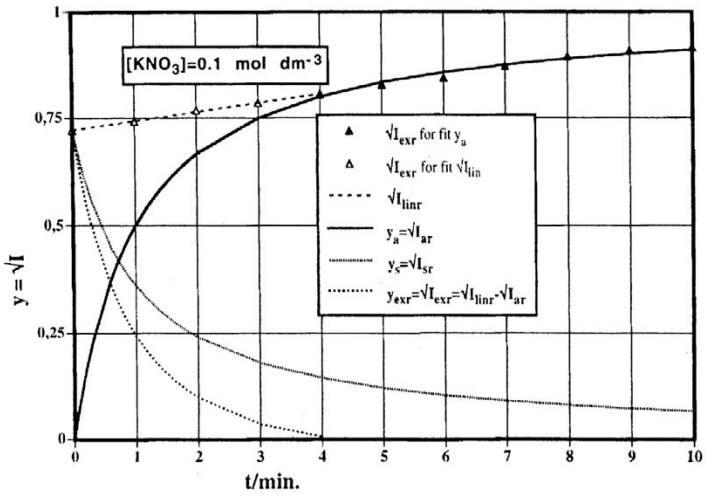

Figure 6. Coagulation kinetics of the sol: [AgI] = 0.04 mol dm^{-3}, [KI] = 0.02 mol dm^{-3}, [KNO_3] = 0.1 mol dm^{-3}. Abscissa: time, t/min. Ordinate: square root reduced absorbency, $y = \sqrt{I_r}$. Experimental points from Figure 2[16]. Fitted straight line: $y = \sqrt{I_{linr}}$. Aggregate formation or coagulation plot (21): $\sqrt{I_{ar}} = \sqrt{I_a}/\sqrt{I_\infty} = y_a$. $\sqrt{I_{ar}} = 1/2$ defines $t_{1/2} = 1$ min.

A convincing support for the proposed theory is the fact that $\sqrt{I_{sr}} \xrightarrow{t \to 0} \sqrt{I_{exs}} = y_s$.

The simplest method is that described in Figure 7, in which a series of experimental points ($1/\sqrt{I_{exr}}$, $1/t$) and point ($1/t = 1$, $1/\sqrt{I_a} = 2$), which were used for fitting I_{ex}, Eq. (22), and the theoretical straight line $1/\sqrt{I_{ar}} = 1 + 1/t_r$, are drawn. The straight line extrapolated to $1/t = 0$ defines the value $\sqrt{I_\infty} = \sqrt{0.354} = 0.595$ and for $1/\sqrt{I_{ar}} = 2$, one obtains $1/t = 1/t_{1/2} = 1.0$/min. or $t = t_{1/2} = 1.0$ min.

In Figure 3,[5] an analogous method is suggested but erroneously based on the supposition that the experimental points ($1/I_{ex}$, $1/t$) can be used for the determination of $t_{1/2}$ instead of the points ($1/\sqrt{I_{ex}}$, $1/t$). The consequence is that $I_a = I_\infty/2$ defines an erroneous value for $t_{1/2}$ because the correct value is obtained by $I_a = I_\infty/4$, which defines correctly $t_r = 1$ and $t_{1/2} = 1$ min. as proved above by Eq. (20).

In the method proposed by Težak and used for many years in our (Zagreb or Težak's) school of colloid chemistry, the »critical« coagulation time was in use for a relative characterization of the coagulation rate. In practice, the

experimental points (I_{ex}, log t) were plotted and by visual interpolation the tangent on the steepest part of the plot, through inflection, was drawn. The intersection of the tangent with the abscissa, *i.e.*, the point for $I_{ex} = 0$, was called the logarithm »critical coagulation time, »log t_{crit}«. It was assumed correctly that the critical coagulation time characterizes the coagulation rate. In the era of slide rulers and visual fitting, the method was very useful for comparison of relative rates in variable coagulator concentrations of different systems. The theoretical interrelation between the experimental critical coagulation time and the coagulation half life was at that time not understood. Its explanation follows.

The first derivative of the function

$$-ln\left(\frac{1}{\sqrt{1/I_{ar} - 1}}\right) = \ln t_r \tag{27}$$

which was obtained from Eq. (21), reads

$$\frac{d\sqrt{I_{ar}}}{d(ln\ t_r)} = \sqrt{I_{ar}} \times (1 - \sqrt{I_{ar}}) \ . \tag{28}$$

At the infelction point, for $\sqrt{I_{ar}} = 1/2$, the slope is $d\sqrt{I_{ar}}/d(\ln t_r)_{infl} = 1/4$ and the equation of the tangent, $\sqrt{I_{ta}}$, through the inflection reads

$$\sqrt{I_{ta}} = \frac{(\ln t - \ln t_{crit})}{4} \ . \tag{29}$$

The intersection of the tangent with the abscissa is the »logarithm critical time, $\ln t_{crit} = -2$«, and the following holds

$$\ln t_{1/2} = \ln t_{crit} + 2 \quad or \quad t_{1/2} = e^2 \times t_{crit} \ . \tag{30}$$

In the present example one obtains again $t_{1/2}$ = 1 min.

It is demonstrated in this way that the value »t_{crit}« characterizes the coagulation process and can serve for determination of $t_{1/2}$ and k_c

Erroneous Half-Life Determination. Many authors have used the method of determination of $t_{1/2}$ based on the estimation of the slope of the plots $t_{1/2} \xrightarrow{t \to 0} dI_{ex}/dt$. The same method was also erroneously proposed in reference[5] and used erroneously in references.[17,18] At high sol concentrations, when $I_0/I_\infty >\approx 1/10$ equals an appreciable fraction of I_∞, the method is inapplicable as proved above. It is approximate in low [AgI] concentrations, if I_0 can be subtracted from I_{ex} as zero effect, when the I_{ex} and I_a plots are practically equal.

The first derivative of Eq. (20) reads

$$dI_{ar}/dt_r = 2 \times \left(1 + 1/t_r\right)^{-3} t_r^{-2} \tag{31}$$

and $dI_{ar}/dt \xrightarrow{t_r \to 0} 0$ holds. The value $I_{lin} = I_{ex} < I_\infty$ cannot give a correct value of $t_{1/2}$. Correct $t_{1/2}$ determination is defined by $I_a = I_\infty/4$ and described by Eq. (20) and Figures 4, 5 above.

All the four methods described are as precise as the constants I_∞, I_0, F, $t_{1/2}$, obtained by fitting of equations (20) and (21), are precise.

The present day availability of fitting programs of any function to any experimental plots makes all the four proposed methods equally convenient. The most straight forward is that described in Figures 4, 5.

It is demonstrated by the present analysis that the light scattering measurements are an excellent tool for quantitative coagulation kinetics investigations. A published experiment[17] analyzed on the basis of Rayleigh's theory strongly supports the correctness of the second order coagulation theory of the formation of big polydisperse aggregates containing hundreds of singlets.

ADSORPTION OF [I^-_{ads}], PEPTIZATION AND »ISOELECTRIC« COAGULATION OF AGED AgI

»Adsorbed I^-_{ads} on AgI versus pI« plots. Three types of experimental plots »adsorbed concentration of [I^-_{ads}] per concentration of [AgI] *vs.* pI *or* pAg«, *or* »γ = [I^-_{ads}]/[AgI] *versus* pI« plots, have been observed to date: (a) Linear plots obtained with freshly precipitated AgI, Figures 3,[15,31] (b) Isotherms having a horizontal saturation region obtained with AgI in the presence of counter ions in their, for coagulation, sufficiently high concentration[11] and (c) curved plots with aged and dried AgI.[19, 20]

The linear plots observed with fresh samples at a low concentration or low ionic strength, I, of counter ions of charge number $z = 1$, *i.e.*, $I = [M^+] <\approx 0.01$ mol dm^{-3}, can be explained in the following way:[15] The first smallest addition of [Ag^+] to the [I^-] solution causes its saturation with $(AgI)_m I^-_n$ complexes. The most abundant complex ions, $(AgI)_2I^-$, act as nuclei or embrya for the growing small stable particles charged with one single adsorbed I^-_{ads} The growth is caused by stepwise addition of [Ag^+] which causes a decrease of [I^-] and ΔpAg and an increase of the intensity of scattered light, I_{ex}. The linear decrease of $\gamma(\Delta pAg)$ and the continuous increase of the intensity of scattered light plots are possible because the growing single stable particles are formed by coalescence of the smaller colliding particles and the

process is accompanied by a decrease of $[I^-_{ads}]$. The plots can be described by the linear function

$$\gamma_I = \Gamma_I^0 \times \Delta pAg \tag{32}$$

where Γ_I^0 is the constant slope which depends on $[M^+]$ and [AgI]. The linear plots were theoretically analyzed in references.[15] The continuous increase of the intensity of scattered light during titration is demonstrated in Figure 2, p. 226[24] in the range $10^{-4} < [AgI]/[mol\ dm^{-3}] < 10^{-2}$.

With coagulated samples of AgI, the observed plots had a saturation region and could be described by[11]

$$\gamma_e = \Gamma_e^0 \times \left[1 - \exp\left(F_1 \times \Delta pAg\right)\right] . \tag{33}$$

The systems obtained at each measured pAg were left over night to equilibrate. The constant, F_1, determines practically the saturation region of γ_e and Γ_e^0 its saturation value. If the change of pAg is fast, *i.e.*, if the system was not left standing over night after each addition of $[Ag^+]$, *i.e.*, at each ΔpAg, the plots were curved with no horizontal saturation region.

The third type of plots are shown, *e.g.*, in Figures 4, 5,[20] 1, 4, 5, 9, 10, 21, 22, 23, 24, 33, 34, 35, 36, 43, 47.[21] They were obtained with well aged and dried samples of [AgI] and were as a rule published as »*surface charge(= charge density = σ_0) against* pI *or* pAg« *or* σ_0[pAg] plots.

Indeterminacy of the σ[pAg] *Plots.* Actually, the same plots were and could be measured solely as plots of the molar quotient »adsorbed quantity of $[I^-_{ads}]$ per amount of [AgI]« or as »$[I^-_{ads}]$/[AgI]=γ versus pI« plots. The equation of transformation reads[22]

$$\sigma_0 = \gamma \times e \times L/(S_0 \times M_{AgI}) \tag{34}$$

where: e is the elementary charge, L the Avogadro-Loschmidt constant, M_{AgI} the molar mass of AgI. The transformation factor contains the specific surface, S_0. For the cited figures, neither the values γ nor S_0 are quoted. No explanation is given for the curvature of the plots, either. For this reason, the charge density function and the curvature are undetermined and the measured γ plot values unknown.[22]

Specific Surface Determination. The authors[19,20] claimed that the S_0 value can be estimated (See Figure 9[20]) by equating the slope of the tangent of the supposed σ_0 plot, in fact of the γ plot, with the electric capacitance of the galvanic cell: »mercury / electrolyte / reference electrode« both for $\Delta pAg \rightarrow 0$. The colloidal system of two phases is in no relation whatsoever, either physical or theoretical, with the galvanic cell that has at least three phases, *i.e.*, two electrodes and electrolyte. For this reason, the equating of the two slopes is impermissible and the S_0 values obtained by the described equating of the slopes are in principle incorrect.

The authors assumed that, after the immersion of the sample in the electrolyte, during the time before the start of titration and during titration S_0 = cons. An independent experimental confirmation of the above assumptions would be absolutely necessary, however, the authors did not offer it. Also, no S_0 values are quoted in the cited two papers.[19,20] In addition, neither data on the crystallographic habitus nor micro- or electron micrographs of the well ages samples have been published. Constancy of the AgI dispersity, *i.e.*, of S_0, during experiment has not been proved and many arguments can be quoted proving that the dispersity, as well as the double layer, of aged AgI change during titration.

Adsorption of Iodide Ions, I^-_{ads}, on Aged AgI. Figures 2, 5, 9,[19] 1, 4, 5, 9, 10, 21, 22, 23, 24, 33, 34, 35, 36, 43, 45, 47,[20] represent formally variation of the »*surface charge density*, σ_0, (ordinate), with pAg (or pH for $Fe(OH)_3$)«, *i.e.*, plots »σ_0(pAg)«. The σ_0 unit is given as $\mu C\ cm^{-2}$ and its dimension is $[\sigma_0] = [Q]\ [l^{-2}]$. The σ_0(pAg) plots were and could be exclusively obtained from experimental γ(pAg) plots which, in turn, were measured by »fast« titration, *i.e.*, by titration when after each addition of $[Ag^+]$ no sufficient time is left to obtain and prove the state of dispersion and adsorption equilibrium. The variable $\gamma = [I^-_{ads}]/[AgI]$ is a dimensionless molar quotient, $[m \times l^{-3}]/[m \times l^{-3}]$.

Determination of $\gamma(\Delta pAg)$ Plots. The actual experiments that served to determine the $\gamma(\Delta pAg)$ plots can be described as follows: To a given quantity, m_{AgI}, of a well aged and dried sample of AgI, a given volume, v, of a solution containing [KI] + $[KNO_3]$ is added. After a given time, the time of supposed equilibration, $pAg_{max} = -\log K_{AgI} - pI_{min}$ is determined potentiometrically. Subsequently, a solution of $AgNO_3$ is added in small portions, *i.e.*, a titration is performed. After each addition the electromotive force, EMF, between a convenient indicator electrode and a reference electrode, is determined and pI or pAg are calculated as a function of the added $[Ag^+]$. The variable parameter $\Delta pAg = pI_0 - pI = pAg - pAg_0$ can be chosen for convenience: the decrease of ΔpAg causes a decrease of γ and σ_0. The parameters pI_0 and pAg_0 are the zero points of adsorption, *i.e.*, the intersections of the plots with the pI or pAg abscissa. Then $\Delta pAg = 0$ when $\sigma_0 = 0$, in fact $\gamma = 0$, and $\log K_{AgI} = pI + pAg = pI_0 + pAg_0$ holds. The ionic product of AgI is K_{AgI}.

An analogous titration plot is measured; however, practically with no AgI present. From the difference between two points on the two plots at constant pAg or EMF, one obtains $[I^-_{ads}]$, *i.e.*, the concentration of adsorbed I^-_{ads} as a function of ΔpAg. The molar ratio, $\gamma = [I^-_{ads}]/[AgI]$, is a function of ΔpAg, namely the function $\gamma(\Delta pAg)$ for $\Delta pAg_{max} \rightarrow \Delta pAg \rightarrow 0$. The rate of the decrease of ΔpAg was neither defined nor quoted for the analyzed plots. When one analyzes the $\gamma(\Delta pAg)$ plots, the rate of titration should not be neglected. The quantity of immersed [AgI] per unit volume of electrolyte can be called or understood as its »concentration«, *i.e.* $\gamma = [I^-_{ads}]/[AgI] = m_{AgI}/vM_{AgI}$.

The reciprocal of γ, *i.e.*, $n = 1/\gamma$, defines the number of [AgI] units on which one I^-_{ads} is adsorbed. Objectively, during the decrease of $\Delta pAg_{max} \rightarrow 0$ it was established only that $[I^-_{ads}]$ decreases while [AgI] = *cons*. The concentration of [AgI] is either equal to the added amount per dm^3 of dry [AgI] or, in the case of direct precipitation, to the precipitated [AgI], *i.e.*, to $[Ag^+]$ added before pI $\approx$ 5 has been reached. Then, [AgI] $\approx$ cons.

The measured decrease of $[I^-_{ads}]$ is a consequence of the reaction:

$$(AgI)_n I^-_{ads} + Ag^+ = (AgI)_{n+1} \ .$$

The surface, in fact the corresponding number, $n = 1/\gamma$, of [AgI] units becomes uncharged when one I^-_{ads} is desorbed, in fact transformed into [AgI] This means that the number concentration of particles, having at ΔpAg_{max} a given quantity of $[I^-_{ads}]$ decreases and the concentration of particles, with partially or fully neutralized $[I^-_{ads}]$, increases. In this way, only the observed continuous decrease of γ with the decrease of ΔpAg can be explained. The smallest particles, stable or singlets, are those charged with the smallest possible charge, *i.e.*, with one I^-_{ads}.

Evidently, the experimental $\gamma(\Delta pAg)$ plot and the corresponding function, $\sigma_0(\Delta pAg)$, are undetermined if either the values S_0 or the measured set of γ values are not quoted or, if the size and form of the particles are not defined or known. Since S_0 was always taken constant in the transformation of the $\gamma(\Delta pAg)$ into the $\sigma_0(\Delta pAg)$ plot, for each [AgI] sample, the real unit of the $\gamma(\Delta pAg)$ plot is unknown but the two plots are proportional.

Iodide Ion Adsorption, I^-_{ads}, on Aged [AgI]. The measured plots of aged samples, γ_a, are, as a rule, neither linear nor they have a saturation region. They can be theoretically represented by the sum, γ_a, of the linear function (32) and the exponential function (33), namely by

$$\gamma_a = \gamma_l + \gamma_e = \Gamma^0_l \times \Delta pAg + \Gamma^0_e \times [1 - exp(-F_e \times \Delta pAg)] \qquad (35)$$

Then the following is possible: (a) after immersion of AgI and before the start of titration a constant part of [AgI] remained unchanged, another part was peptized and a part of the peptized AgI was coagulated. (b) During the titration, *i.e.*, during the decrease of ΔpAg, practically in $0.01 \leq [KNO_3]/(mol\,dm^{-3}) \leq 1$, no further peptization takes place. In $1 \times 10^{-4} \leq [KNO_3]/(mol\,dm^{-3}) \leq 1 \times 10^{-3}$, the plots are explained by peptization and coalescence during titration.

Indeterminacy of the $\sigma_0(\Delta pAg)$ Plots. The $\sigma_0(\Delta pAg)$ plots[19,20] are undetermined[22] since they are published without the quoted, supposedly constant, value of S_0 on the basis of which they were calculated and since the $\gamma(\Delta pAg)$ function is not defined by a second ordinate scale. For this reason, in Figures 9–13, the real unit for γ is unknown or relative.

Inconstancy of the Specific Surface. The transformation of the experimental $\gamma(\Delta pAg)$ plots into the undetermined $\sigma_0(\Delta pAg)$ plots has been performed under the erroneous assumption that S_0, *i.e.*, dispersity, is constant. The supposed constancy of dispersity has been neither checked nor proved experimentally.

However, from heterogeneous exchange experiments of many precipitates, also of different [AgI] samples,[23] it follows that changes of the supernatant electrolyte concentration, or simply any immersion of the dried precipitate in an electrolyte, under various conditions, cause a complete dissolution of the solid followed by formation of a precipitate of different dispersity, occasionally also of different crystallographic modification. This phenomenon is called peptization and recrystallization. In addition, the unlinearity of the $\gamma(\Delta pAg)$ plots is a direct proof that the dispersity changes during titration. It is more than certain that the dispersity of aged and dried samples of [AgI] changes after its immersion into the experimental electrolyte and during titration. An additional proof that the dispersity changes during the titration is the increase of the intensity of scattered light or absorbency during the titration of fresh sols with Ag^+ (See Figure 2, Ref. 24). This can also be observed with aged samples.

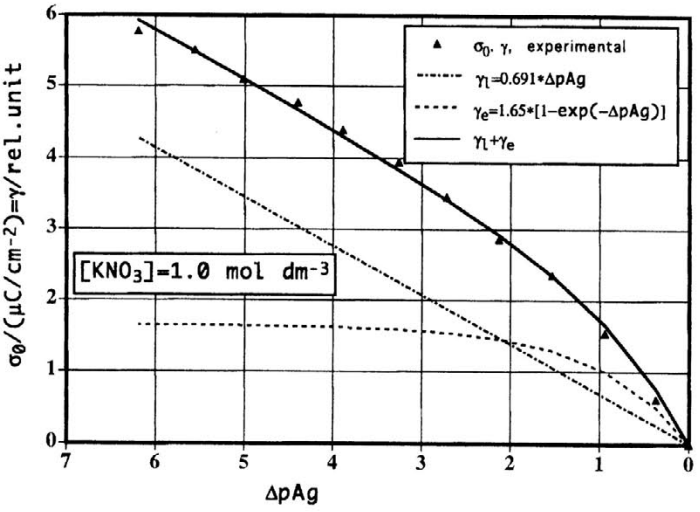

Figure 9. »Charge Density, σ_a, σ_e, σ_I/(mC/cm^{-2}), *versus* ΔpAg«, actually »γ_a, γ_e, γ_I = $[I^-_{ads}]/[AgI]$ *versus* ΔpAg« plots of aged AgI in $[KNO_3]$ = 1.0 mol dm^{-3}. Constants: preset $\Gamma_I^0 = 0.2$; $\Gamma_e^0 = 5.75$, $F = 0.164$; obtained by fitting (35) to experimental points of Figure 5[21]. Due to the high $[KNO_3]$, at the beginning of titration a greater part of [AgI] is already peptized and coagulated and a smaller part peptized only. During titration the smaller peptized part coalesces and, therefore, $\gamma_e^0 < \gamma_I^0$.

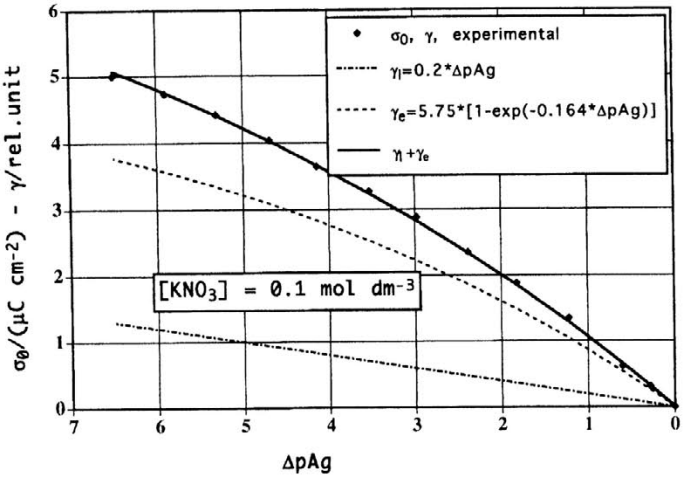

Figure 10. »Charge Density, σ_a, σ_e, $\sigma_I/(\mu C/cm^{-2})$, *versus* ΔpAg«, actually »γ_a, γ_e, γ_I = $[I^-_{ads}]/[AgI]$ *versus* ΔpAg« plots of aged AgI in $[KNO_3]$ = 0.1 mol dm^{-3}. Constants: preset $\Gamma_I^0 = 0.2$, $\Gamma_e^0 = 5.75$, F = 0.164 obtained by fitting (35) to experimental points of Figure 5[21]. Due to the slightly higher $[KNO_3]$, at the beginning of titration a greater part of [AgI] is assumed to be already peptized and coagulated and a smaller part peptized only. During titration the smaller peptized part coalesces and, therefore, $\gamma_e^0 > \gamma_I^0$.

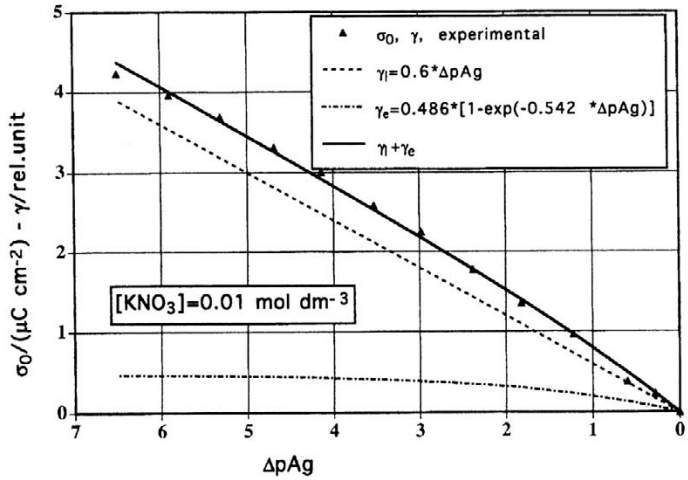

Figure 11. »Charge Density, σ_a, σ_e, $\sigma_I/(\mu C/cm^{-2})$, *versus* ΔpAg«, actually »γ_a, γ_e, γ_I = $[I^-_{ads}]/[AgI]$ *versus* Δ*p*Ag« plots of aged AgI in $[KNO_3]$ = 0.01 mol dm^{-3}. Constants: preset $\Gamma_I^0 = 0.6$, $\Gamma_e^0 = 0.486$, F = 0.542 obtained by fitting (35) to experimental points of Figure 5[21]. Due to the slightly lower $[KNO_3]$, at the beginning of titration a smaller part of AgI is already peptized and coagulated and a bigger part peptized. During titration the peptized part coalesces and, therefore, $\gamma_e^0 < \gamma_I^0$.

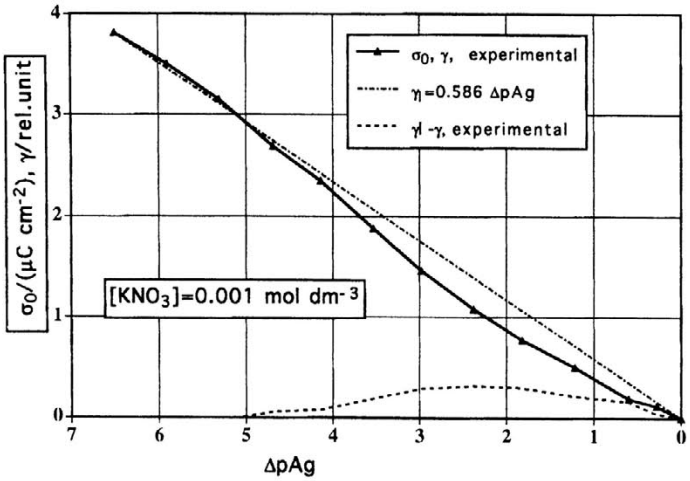

Figure 12. »Charge Density, σ_a, σ_e, $\sigma_1/(\mu C/cm^{-2})$, *versus* ΔpAg«, actually »γ_a, γ_e, $\gamma_1 = [I^-_{ads}]/[AgI]$ *versus* ΔpAg« plots of aged AgI in $[KNO_3] = 0.001$ mol dm^{-3}. Constants: preset $\gamma/\Delta pAg_{max} = \Gamma_1^0 = 0.586$, $\gamma_1 - \gamma_{experimental}$. At the beginning of the titration due to the low $[KNO_3]$, peptized AgI only is present and no coagulation but coalescence only take place. At $\Delta pAg <\approx 5$ additional AgI, $\gamma_1 - \gamma_{experimental}$ peptizes and coalesces.

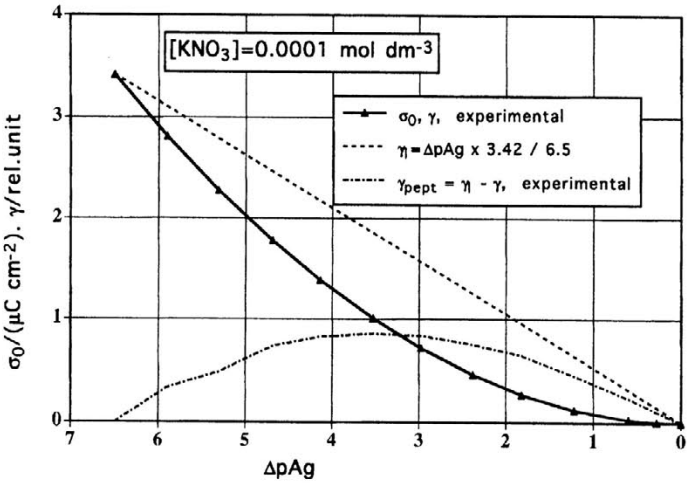

Figure 13. »Charge density, σ_a, σ_e, $\sigma_1/(\mu C/cm^{-2})$, *versus* ΔpAg«, actually »γ_a, γ_e, $\gamma_1 = [I^-_{ads}]/[AgI]$ *versus* ΔpAg« plots of aged AgI in $[KNO_3] = 0.0001$ mol dm^{-3}. Constants: preset $\Gamma_1^0 = 0.526 = \gamma_{max}/\Delta pAg_{max}$, $\gamma_1 - \gamma_{experimental}$ obtained by fitting (35) to experimental points of Figure 5[21]. At the beginning of titration, due to the low $[KNO_3]$ peptized AgI only is present and coalescence only takes place and no coagulation. At $\Delta pAg_{max} < 6.5$ additional AgI, $\gamma_1 - \gamma_{experimental}$ peptizes and coalesces.

At the start of titration, the factors Γ_e^0, Γ_1^0 and F for each plot depend on the amount of unchanged, peptized and not coagulated, as well as on coagulated [AgI], and on their change during titration or the decrease of ΔpAg. The same factors depend, therefore, primarily on [KNO_3] and on ΔpAg_{max} if [AgI] = cons. If at the start of titration all of AgI is peptized and coagulated then during the titration no coalescence occurs and it must be $\gamma_1 = 0$ and $\Gamma_1^0 = 0$. If during titration the peptization and coalescence take place, the three parameters are not constant. Independent experiments would be necessary to estimate the amounts of unchanged, peptized and coagulated AgI at the start of titration.

From the published plots (*e.g.*, See Figures 2, 5, 9;[19] 1, 4, 5, 9, 10, 21, 22, 23, 24, 33, 34, 35, 36, 43, 47[20]) it can be concluded that the higher the concentration of the counter ion, [M^+], or the value ΔpAg_{max}, the higher are the σ_0, in fact the γ_a, plots. This means that [I^-_{ads}] and the peptized and coagulated part of [AgI] are increased. It should be concluded, therefore, that the unlinearity of the same plots and their increase with the increase of [KNO_3] are caused by peptization of at least a part of AgI, while the other part is already peptized and fully or partially coagulated at the beginning of titration. The smallest peptized sol particles coalesce during titration and produce bigger particles.

Analysis of the γ(ΔpAg) Plots. In order to support experimentally the explanation given by Eq. (35), several points on each published plot of Figure 5,[20] obtained at different concentrations of KNO_3, have been measured. Since the amounts of the total, coagulated and peptized AgI are not known, probable or possible values for Γ_1^0 were selected in advance. By an appropriate fitting program, the parameters Γ_e^0 and F_1 were determined. Usually, all three constant, Γ_1^0, Γ_e^0, F_1, cannot be obtained directly by fitting. One of them must be selected in advance or it should be determined by an independent method.

It follows from coagulation experiments that the coagulation rate increases with coagulator concentration. It is negligible in low [KNO_3] $<\approx$ 0.001 mol dm^{-3}, in medium concentrations it increases and it is rapid in high [KNO_3] $>\approx 0.01 \times$ [mol dm^{-3}] concentrations.

The quotient »variable coagulation rate/maximal coagulation rate« is occasionally called »stability factor«. It represents a broken line. Concentration of the intersection of the constant and variable lines with [M^+] defines *c.c.c.* The peptization rate depends also on [KNO_3] and ΔpAg_{max}.

With the aid of the three parameters the linear Eq. (32), γ_1, the exponential Eq. (33), γ_e, and their sum Eq. (35), the $\gamma_a = \gamma_1 + \gamma_e$ plots, were drawn in Figures 9, 10, 11, 12 for each [KNO_3]. The points measured on the published plots of Figure 5[20] are also inserted. This means that the figures formally represent the plots:

»σ_0, σ_e, σ_l/[μCcm^{-2}] *versus* ΔpAg« and actually »γ_a, γ_e, $\gamma_l = [I^-_{ads}]$/[AgI]/(rel. unit) *versus* ΔpAg«. The units of γ_a, γ_e, γ_l are unknown for the reasons described above.

It has been shown that the measured $[I^-_{ads}]$ on aged and dried [AgI] by fast titration is equal to the sum of $[I^-_{ads}]$ adsorbed on the peptized, coalesced and coagulated parts of aged [AgI]. It has been also demonstrated that the surface charge or charge density, σ_0, is an erroneous and wrong variable for the definition of $[I^-_{ads}]$, which is not in accordance with SI recommendations.

In all five concentrations of $[KNO_3]$ at ΔpAg_{max}, $\gamma_{amax} = \gamma_{emax} + \gamma_{lmax}$ is proportional to the sum of the peptized, coalesced and coagulated forms of AgI. The lower is the $[KNO_3]$ at the beginning of titration, the lower are the peptized and coagulated parts of AgI. In the two lowest $[KNO_3]$, before and during titration, practically no coagulation takes place but peptization and coalescence only. The following observations and conclusions can be made.

In $[KNO_3] = 1$ mol dm^{-3} (Figure 9), due to the high $[KNO_3]$ at the beginning of titration the relatively low $\Gamma^0_l = 0.4$ was selected in advance and by fitting $\Gamma^0_e = 3.6$ and $F = 0.403$ were obtained. If, at the beginning of titration, no peptized but partly coalesced plus coagulated [AgI] is present, then $\Gamma^0_l = 0$ and by fitting one obtains $\Gamma^0_e = 7.5$ and $F = 0.228$. During titration, an additional part of coalesced [AgI] coagulates.

In $[KNO_3] = 0.1$ mol dm^{-3} (Figure 10), due to the slightly higher $[KNO_3]$, at the beginning of titration a greater part of AgI is already peptized and coagulated and a smaller part peptized only. During titration the smaller peptized part coalesces and, therefore, preset was the probable or possible $\Gamma^0_l = 0.2$ and the constants obtained by fitting are $\Gamma^0_e = 5.34$; $F_e = 0.184$. The γ_e plot is higher than the γ_l plot, $\gamma_e > \gamma_l$.

In $[KNO_3] = 0.01$ mol dm^{-3} (Figure 11), the coagulation is very slow and a small part of [AgI] is coagulated at the start of titration. Due to the slightly lower $[KNO_3]$ at the beginning of titration, a smaller part of $\gamma_e < \gamma_l$ is already peptized and coagulatedd and a bigger part is peptized only. During titration the bigger, peptized part coalesces and, therefore, $\gamma_e < \gamma_l$. With the preset $\Gamma^0_l = 0.6$, the constants are: $\Gamma^0_e = 0.487$, $F_e = 0.543$.

In $[KNO_3] = 0.001$ mol dm^{-3}, (Figure 12), the γ_{exp} plot is convex relatively to the γ_l plot. Before the start of titration the part γ_l of [AgI] is peptized and an additional part, the part $\gamma_l - \gamma_{exp}$, increases up to its maximum. The increase is caused by peptization of additional AgI. After the maximum, coalescence takes place and causes the decrease of $\gamma_l - \gamma_{exp}$. Consequently, $\Gamma^0_e = F_e = 0$. If coalescence of the peptized part only would occur the γ_l plot would be linear with $\Gamma^0_l = \gamma_{max}/\Delta pAg_{max} = 0.586$.

In $[KNO_3] = 0.0001$ mol dm^{-3} (Figure 12), the plots are similar to those of Figure 11. Due to the lowest $[KNO_3]$ additional peptization starts at the beginning of titration, *i.e.* the $\gamma_l - \gamma_{exp}$ plots starts to increase at the beginning of titration and its maximum is higher.

The Radius of Stable AgI Particles and Singlets in »Isoelectric« Coagulation. In titration of fresh sols, the experimental decrease of γ_1 with ΔpAg is linear and it holds (Equation 14,[21] π = Ludolf's constant, d = density)

$$r_s = \sqrt[3]{3 \times M_{AgI}/(4 \times \pi \times L \times d \times \Gamma_I^0 \times \Delta pAg)} \qquad (36)$$

This means that the (average) radius of stable particles, r_s, continuously increases with the decrease of ΔpAg. The proof is the continuous increase of I_s (See, *e.g.*, Figure 2[24]). A continuous increase is possible only if the colliding particles are not rigid spheres. At each new ΔpAg, their size is in a transient dynamic equilibrium, the particles collide repeatedly and at each collision they coalesce and split off and form particles of sizes $r_{min} \leq r_{average} \leq r_{max}$. As long as the particle diameter is $2r < 1/\kappa$, the minimal distance between the surfaces, the distance of closest approach, between two particles is $2/\kappa - 2r > 0$. See Figure (14a). The electrostatic repulsion energy is bigger than the kinetic energy of Brownian collisions. The short range Van der Waals forces are ineffective because the surfaces do not come in contact. The particles cannot coalesce and are colloidally stable.

According to the elementary version of the Debye-Hückel theory, the most probable, or optimal average distance between two equal charges, also between two equal charges on two colloidal particles (See Figure 14b) in Brownian motion, is $2r = 1/\kappa$. Then, the repelling electrostatic forces are equal to the forces determined by concentration. If, at $\Delta pAg < \Delta pAg_{limit} = 0$, the radius of the stable particles becomes $r_{st} \geq 1/\kappa$ (See Figure 14c), the two particles collide, the surfaces come in contact, and the short range Van der Waals forces are effective. The two particles produce, by coalescence, a new particle of $r_{st} \geq 1/\kappa$, which would be charged with two charges. However, the repelling force between the two charges is now stronger than the adsorption force. For this reason, one charge will be desorbed. The new particles, now charged with a single charge, can collide repeatedly (See Figure 14c). If, by repeated collisions, eight ($=2^3$) particles of $r_{st} = 1/\kappa$ produce one spherical particle of diameter $2r_{si} = 2/\kappa$, it cannot increase further by coalescence and the same particle becomes one singlet of the future aggregates (See Figure 14d). The observed continuous growth of stable particles evidenced by the continous increase of scattered light intensity is possible only if transient equilibrium exists at each established ΔpAg.

The attracting van der Waals forces between the surfaces of two singlets are effective in collisions but they cannot cause coalescence. A big part of the surface is outside the sphere of $r_{si} = 1/\kappa$. For this reason, singlets can repeatedly collide, *i.e.*, their surfaces come in contact and form aggregates of increasing number size, *i.* (14d, e)

The empty space between the singlets is filled with intermycellar liquid. The density of I^-_{ads} would be too high in the aggregates and one could expect

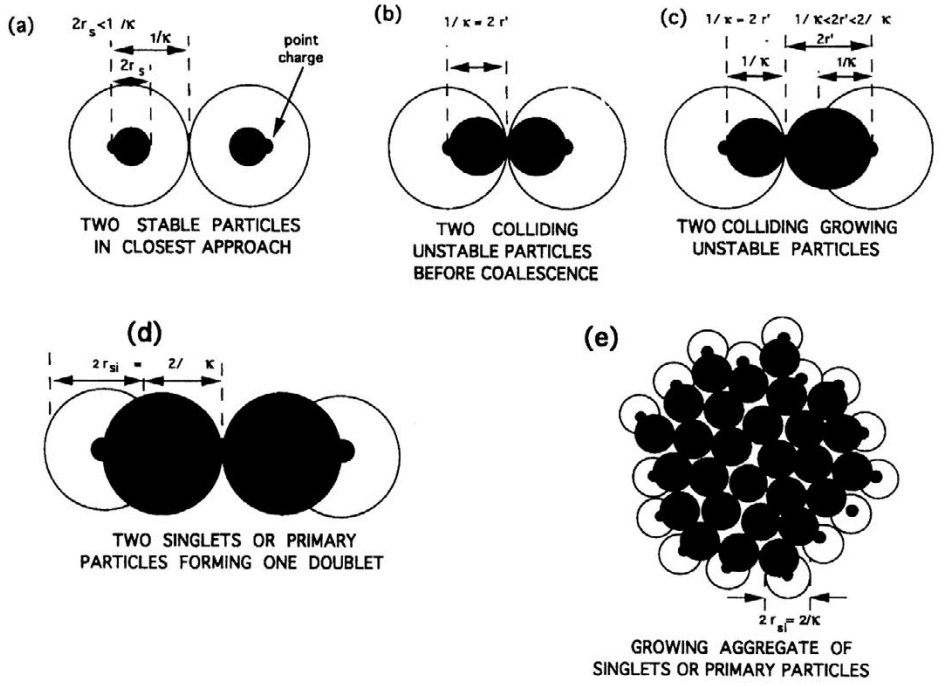

Figure 14. Growth of small stable particles, formation of singlets by coalescence and coagulation during titration (schematic). Due to collisions by Brownian motion:
(a) Two Stable particles of diameter $2r < 2/\kappa$ charged with 1 elementary point charge each in closest approach. Contact of particle surfaces and consequently coalescence are impossible. The electrostatic repulsion energy is bigger than the Brownian collision energy.
(b) Efficient collision of two particles of $2r = 1/\kappa$. The electrostatic repulsion energy is smaller than the Brownian motion kinetic energy, the surfaces are in contact and the Van der Waals forces cause coalescence of particles.
(c) Resulting particle diameter is $1/\kappa \leq 2r \leq 2/\kappa$ and one elementary charge after coalescence will be desorbed.
(d) Efficient collision of singlets of $2r = 2/\kappa$. The singlets are charged with one elementary charge each. The electrostatic repulsion energy is smaller than the Brownian motion kinetic energy and the Van der Waals forces cause formation of porous aggregates in »isoelectric« coagulation. The process is possible in the »isoelectric« region when $0 > \Delta pAg > -2$ or $6.5 > pAg > 4.5$. Some charges are desorbed.
(e) A growing aggregate formed by repeated collisions of singlets of $2r = 2/\kappa$. The process is called aggregation or coagulation. The particles on the surface are charged, those inside the aggregate are not charged. Note: The possible influence of the dielectric constant of dense particles upon the symmetry of the ionic atmosphere is neglected!

that with the decrease of $\Delta pAg \rightarrow 0$ and the increase of the number size, i, some I^-_{ads} would be desorbed, *i.e.*, γ would decrease (See Figure 14e). When the aggregates start to sediment, the further growth caused by Brownian collisions becomes negligible and the scattered light intensity starts abruptly to decrease.

In the absence of coagulators, is $I <\approx 1 \times 10^{-3}$ mol dm^{-3}, and it causes the »isoelectric« coagulation (See. *e.g.*, Figures 13, 14[6]) by passing $pAg > pAg_{limit} = 6.5$ to $pAg < 6.5$ or $\Delta pAg > \Delta pAg_{limit} = 0$ to $\Delta pAg < 0$ and it causes the transition $[I^-_{ads}] \rightarrow 0 \rightarrow [Ag^+_{ads}]$. In the absence of coagulators, it causes a change of the negative electrophoretic mobility of stable particles to the positive electroosmotic transport across a membrane. In the presence of coagulators, it causes transition of the negative to the positive electroosmotic transport of the electrolyte.

The passing of the negative stability limit of $pAg_{limit} = 6.5$ causes an increase of the stable particle diameter $2r_s < 1/\kappa = 9.6$ nm (Figure 14a), to $2r' = 2/\kappa$ (Figure 14b). The particles of $2r' = 2/\kappa$ are unstable. In repeated collisions they coalesce till their diameter becomes $2r_{si} = 2/\kappa$. Such particles are now singlets of the future aggregates (Figure. 14d, e).

From Figure 1[21] it follows that in $I \leq 1 \times 10^{-3}$ mol dm^{-3} $1/\kappa >\approx 9.6$ nm, when $\Delta pAg \rightarrow \Delta pAg_{limit}$. In the »isoelectric« coagulation region, $\Delta pAg < \Delta pAg_{limit} = 0$ or $pAg < pAg_{limit} = 6.5$, the radius of the unstable particles increases in the range $2.07 \rightarrow r'/nm \rightarrow 4.62$ and the number of AgI units per one I^-_{ads} increases in the range $571 \geq 1/\gamma \geq 6349$. By repeated collisions and coalescence, the particles increase till they become singlets of $r_{si} = 1/\kappa = 9.6$ nm and $1/\gamma = 50782$. The singlets coagulate. Stirring causes a momentous formation of visible aggregates, which practically do not scatter light, I_a. Abruptly, I_a starts to decrease. After the standing of the system for several minutes, all of the AgI sediments and the liquid above the sediment is clear and $I_a \cong 0$ (See Figure 2[31]).

It follows that the bigger size of singlets in »isoelectric« coagulation is determined by the low ionic strength. The smaller size of singlets in counter ion coagulation is determined by the high ionic strength of the coagulating 1–1 electrolyte that is equal to its concentration or to the concentration of the coagulating counter ion of $|z_\pm| \geq 2$. The concentration of the added coagulating counter ion of $|z_\pm| \geq 2$ electrolyte is very low and, practically, it does not increase the low ionic strength of the stable sol to which it was added.

One could check the proposed theory by independent determinations of dispersity, *e.g.*, by light scattering or electron microscopy or other particle size measurements performed during the titration in the presence of aged AgI. No data on the dispesity, *i.e.*, on particle and aggregate size and crystalographic modification are given for the aged samples and their reactions in references.[19,20]

ELECTROKINETIC PHENOMENA AND SURFACE POTENTIALS

Electrochemical experiments that can give information on the double layer structure, *i.e.*, on the charge distribution and its potentials are electrokinetic, *i.e.*, electrophoretic and electroosmotic experiments. A systematic comparison of point charge-, homogeneous charge-, Gouy-Chapmann-, ion-exchange-, ζ-potential, generally of double layer potentials, with electrokinetic experiments is published in reference[16] where it is shown that the point charge double layer model can be successfully used for the explanation of electrokinetic phenomena.

Electrophoresis can be described as follows. If stable particles move between two charged electrodes of a Galvanic cell in the direction towards the cathode they are electrophoretically negative and their negative mobility can be measured. They are positive if they move in the opposite direction. The charges of the electro negative particles are adsorbed anions, those of the positive ones are adsorbed cations.

It is a generally adopted present-day practice to transform experimental electrophoretic mobilities into ζ-potentials using Smoluchowski's, or exceptionally, Henry's ζ-potential equations.

Calculation of ζ-potentials using Smoluchowski's or Henry's ζ-potential equations is not justified for physical reasons. Smoluchowski's model are cylinders of the lengths and the radii that are big, $l >> r >> 1/\kappa$. Henry's model are spheres of radii of $r > 1/\kappa$. The surfaces of both kinds of particles are assumed to be charged with a homogeneous charge. The real stable AgI particles are small spheres of $r < 1/\kappa$ each charged with one single I^-_{ads}. One single I^-_{ads} cannot be homogeneously spread over the surface of small particles.

Electrokinetics of Coagulated AgI. Membranes can be prepared with coagulated samples of AgI and electrokinetic measurements can be performed by electroosmotic techniques only. Electrophoretic techniques are impossible because sedimentation of aggregates is too fast. Smoluchowski's ζ-potential formula, used for the calculation of the ζ-potential in membranes, is based on the model of long homogeneously charged capillaries having radii of $l >> r >> 1/\kappa$. Actually, the capillaries should be of macroscopic dimensions.

Obviously, Smoluchowski's model for membranes and real membranes prepared with coagulated AgI are incompatible. The space between the singlets in membranes is filled up with liquid and ≈150 singlets are charged with a single I^-_{ads} only.

Calculation of the ζ-potential from electroosmotic measurements using Smoluchowski's model cannot represent the real situation of one elementary charge per ≈150 spherical singlets in membranes. The membranes are formed from an enormous number of aggregates.

Smoluchowski's and Henry's models of particles and membranes are inapplicable to the small stable AgI particles and aggregates in membranes described in Figures 2.1, 2.2, 3, 14. Neither are stable particles big cylinders or spheres, nor large channels exist in the membranes.

The charge of a single I^-_{ads} cannot be homogeneously spread over any surface. The idea of homogeneous spreading of I^-_{ads} over a surface contradicts the atomistic principle of matter. The homogeneous spreading of ions on surfaces is, therefore, for physical principles absolutely impossible. The correct model for single I^-_{ads} adsorbed on colloidal particles and in colloidal membranes can be only the point charge model[21] analogous to the point charge model of the Debye-Hückel theory. According to Figure 3[16], the Debye-Hückel potential functions, calculated using the point charge model, are higher at larger distances than the Gouy-Chapmann potentials that start to decrease at the surface. At the surface charged with a constant surface charge density, the ion cloud and the homogeneous Gouy-Chapmann potentials are equal, $\psi_{\text{ion cloud}} \xrightarrow{\text{distance} \to 0} \psi_{\text{Gouy-Chapmann}}$(See Figure 3).[16]

It is incredible that the great majority of colloid chemists at the end of the 20-th century did not realize that adsorbed ions in the double layer are charged atoms which cannot be homogeneously spread over any surface and that the idea of homogeneous spreading of ions on a surface contradicts the atomistic principle of matter. For the same reason, the Stern, Gouy-Chapman and other »electrical« homogeneous charge models, which are applicable to polarizable electrodes, are inapplicable in colloid chemistry. Equal values of ζ-potentials, expressed by the mV as unit, do not mean equal structures of the double layer, especially not if they are measured by the different electrophoretic and electroosmotic techniques.

It is obvious that the present day explanation and understanding of the slipping process of the electrophoretic mobility and electroosmotic transport are based on models that do not describe the experimental systems realistically, and that they should be changed, in principle.

COLLOIDAL CRYSTALS

Ordering phenomena of polymer latex particles were observed by Ise and collaborators.[26,27] The ordered system is declared by the authors to be ionic and inhomogeneous and it is called colloidal crystal. The micro photographs of colloidal crystals are shown in Plates 1, 2. and Figures 1, 2.[26] The photographs consist of many symmetric hexagons of one central point surrounded by six other central points. The points are the photographed particles. The packing of colloidal crystals was proved to be a body and face centered cube depending on the latex concentration.

Colloidal crystals are a new type of systems that can contribute towards a better understanding of the point charge double layer model. The latter is based on the Debye-Hückel theory of ionic interactions in electrolytes.

The purpose of the proposal of the theory of colloidal crystals is to demonstrate that the experimental colloidal crystals can be considered a realization of the quasi crystals.[28,29] The theory of quasi crystals has been proposed as a theory that is complementary to the Debye-Hückel theory of electrolytes.[A3] Its elementary lattice is face centered cubic.

According to the quais crystal theory, there are in the centers of the planes of a face centered cube six ions, and in the corners eight. In the body centered cube, besides the eight charges in the corners, there is one charge in the center. For theoretical considerations of colloidal crystals, ions of one sign can be replaced by charged particles.

Figure 15. shows the projections of particles in the simple, body and face centered cubes. The projections are on the (111) or photograph plane, perpendicular to a cube diagonal and to the microscope axis.

The photographed patterns or projections of particles are symmetrical hexagons of one particle in the center surrounded by six particles in the corners. The patterns in the simple, the body centered and the face centered cubes are equal.

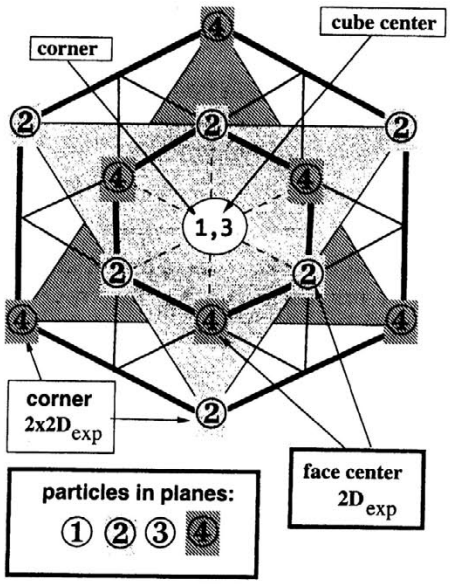

Figure 15. Projection of particles in planes ①, ②, ③, ④, on plane (111) in simple, *sc*, body, *bcc*, and face centered, *fcc*, cubes. The distances between the planes ① – ② and ② – ④ are one third and between the planes ① – ③ one half of the cube diagonal. Particle ① is in the front corner and particle ③ is in the cube center on the perpendicular diagonal. Particles in the small hexagon, ②$_{small}$ and ④$_{small}$, are in face centers and the particles in the big hexagon, ②$_{big}$ and ④$_{big}$, are in cube corners.

The cube corners, body and face centers are in four planes, labeled ①, ②, ③, ④. The distance between planes ① – ② and ② – ④ is one third, and the distance between ① – ③ is one half on the cube diagonal. The cube center is in plane ③. The projections of corners in one plane are triangles of equal sides, $②②②_{big}$ and $④④④_{big}$. The face centers are in two layers forming triangles. Their projections are $②②②_{small}$ and $④④④_{small}$. The distances, $② - ④_{small} = 2D_{exp}$ are projections of halves of the cube edges and distances $② - ④_{big} = 2 \times 2S_{exp}$ are projections of the edges.

The originally proposed lattice of quasi crystals (See Figure 1[30]) is a face centered cube. In the corners there are eight, and in the centers of the faces six charges of one sign. Charges of opposite sign are in the half-point of edges. In the same cubes, besides single elementary ion charges, pairs of charges separated for small distances, l_{ion}, can be found. The eight charges in the half-points of the edges plus pairs of charges replace the ion cloud of the Debye-Hückel theory. Dilution of the electrolyte causes $l_{ion} \rightarrow 0$ (See Figure 2),[30] which corresponds to neutralization or annihilation of the pairs of charges of opposite sign separated for l_{ion}. Equivalent to annihilation is the expulsion of the electrolyte or the pairs of charges replacing it. Expulsion will also occur if the number of elementary charges in the lattice points, *i.e.*, on particles, is big as compared with the number of charges constituting pairs.

Colloidal crystals can be considered analogous to electrolytes. The charges on particles are of one sign, and the ions of opposite sign are in the ion cloud, in the space between the particles.

Before the ordering of the latex, since the number of elementary charges on particles is very big ($>10^4$), also the concentration of the counter ions is very big. During the formation of the macroscopic crystal, each new elementary lattice element ads 4 particles into the last layer of elementary lattice elements in the plane (111): 1 in the point ① and 3 in the points $②_{small}$. The remaining particles are already built into the (111) layer.

The extremely big number of charges on the particles causes, during ordering, expulsion of the 1–1 electrolyte impurity, which unavoidably remains after purification of the latex with ion exchangers. It causes the formation of the experimentally observed disordered region in the system.

The systems of colloidal crystals and of Debye-Hückel quasi crystals are face centered cubes. Of the former also body centered cubes in lower latex concentrations. The projections of simple, body and face centered cubic lattices are equal symmetric hexagonal patterns of one point surrounded by six others.

It follows that the colloidal crystals can be considered an experimental realization of the proposed quasi crystal lattice of the Debye-Hückel theory.

CONCLUSION

Published experimental results, including the newest, have been used to develop and check theories of colloid chemistry. The theories are of particle formation, of particle growth, of coagulation kinetics of small (up to six) and big (hundreds) of singlets, of charge formation on particles, of double layer structure and potentials, of electrokinetic phenomena, of adsorption of potential or constitutive ions on the surface and exchange of counter ions in the ionic cloud.

Old and, especially, new results that served the same purpose of developing new theories were published mostly by very prominent colloid chemists and laboratories. They were obtained by classical, usually modernized and sophisticated techniques. The present paper threats primarily the silver iodide system, and also other ionic inorganic systems and some organic latices. The authors of some recent experimental observations did not, or were unable to explain quantitatively either the old or the newly published results using the conventional theories.

It is claimed in the present paper that the conventional theories of the field were practically never supported quantitatively by experiments and that the experimentally not supported theories should be replaced by new theories. Some proofs of the errors of the conventional theories are described in reference[16] and in the present paper.

Some new theories have been proposed and published by the author through many years in a sequence of papers. The main common principle incorporated into the author's theories is the point charge double layer model and the theory of second order processes as applied for the process of coagulation. The point charge double layer model is analyzed on the basis of the classical Debye-Hückel theory of electrolytes. All the theories of the present author are applications of the generally accepted elementary laws or theories, *e.g.*, the law of Coulombic potentials around ionic point charges, the law of their summation or superposition, the Debye-Hückel theory of ionic interactions in electrolytes, second order reaction theory, theory of ion exchangers, theory of heterogeneous exchange and others. This means that the author's theories were developed by the deductive method and cannot be considered hypothetical or speculative.

Speculative are usually theories developed by the inductive method, especially if the resulting equations can neither be checked by known experimental results, nor by experiments that could be hypothetically discovered in the future. The same elementary principles or theories as applied for colloids are confirmed by available experiments, since they have been developed with the purpose of explaining experimental results. Not a single of the applied elementary theories is of the author's own making, as claimed by a referee of a part of the present paper. However, it is certainly true that all applications of the same elementary principles or theories by the author are original.

The experimentally not confirmed conventional theories are based exclusively on the homogeneous charge double layer model and on the undetermined charge density function.

It must be pointed out that the homogeneous charge double layer structure is in contradiction with the atomistic principle of matter. Adsorbed ions, *i.e.*, charged atoms, cannot be spread homogeneously on surfaces. It is incredible that the present day colloid chemists have not realized this fact.

The basis of the homogeneous double layer model is the surface charge density function. It is undefined since, as a rule, the shape and size of the sol particles are not defined.

Calculation of ζ-potentials from electrophoretic and electroosmotic experimental results using Smoluchowski's ζ-potential equation, since based on the homogeneous double layer model, is for the same reasons unfounded.

The predominantly cited coagulation kinetics theory in the literature is that of Smoluchowski (1916). Although, at its start the same is a binary collision of colloidal particles theory its resulting equations are not of second order as they, consequently, should be. Equations of this theory were never quantitatively confirmed by experiments. In principle, the same is a theory of formation of small aggregates containing several particles only and cannot be applied for an analysis of coagulation of experimentally observed big aggregates of hundreds of primary particles.

Many referees of the author's papers have criticized them in their negative reports. Some editors rejected the author's papers because of such negative reports. Afterwards, the criticized papers were published because the author could, for every point of negative criticisms, convince the editors that the criticisms were, as a rule, subjective opinions of the referees, that they were scientifically unfounded and that they were not confirmed experimentally. Although the author's papers were later published in another journal, not a single criticism was published in the past fifteen or more years.

Author's replies to older published criticisms are discussed in reference[12,A6] and many points of criticisms were proved incorrect also in the published versions of the previously criticized papers.

An interesting fact should be stressed. Practically, no published discussions and criticisms of the conventional theories have been cited in comprehensive treatises on colloid chemistry.[25,35,36] *E.g.*, the subject »point charge« cannot be found in the subject indexes. Also, the criticisms of the theories of the present author[A6] have not been quoted.

Many points of the criticism and many experimental features expressed by the author and described in the present paper have been already published among other also in Refs. 24 and 35.

LIST OF SYMBOLS

B_s, B_i, B_v	proportionality constants of the Rayleigh's light scattering theory for: stable particles, aggregates defined by number sizes, i, defined by volume, v.
$[M^0]$, $[M^z]$	constant of equation (18), molar concentration of an ion of charge number $\pm z$
d	density
e	elementary electron charge
EMF	electromotive force
F	constant defining: the slope of (22), (23); of the exponential γ functions (32), (33)
i_r	number of singlets in radius of aggs.
i, i_a, i_0, i_{max}, i_{min}	aggregate number sizes: variable, variable, defining the histogram width, average, maximal, minimal
I	ionic strength
I_0, I_a, I_{ar}, I_{ex}, I_{exs}	intensity of scattered light: at $t = 0$, on aggregates, relative on aggregates, experimental, on stable particles
I_{lin}, I_{linr}, I_s, I_{sr}, I_{ta}, I_∞	intensity of scattered light: of the linear part of (22), (23), (24), relative, on stable particles, on stable particles relative, of the tangent (29), experimental at $t \to \infty$
j	parameter $1 \leq j = i \leq i_0$ defining n_i for any $i_{min} \leq i \leq i_{max}$
k	Boltzmann constant
k_c	second order coagulation rate constant
K_{AgI}	ionic product of AgI
l, l_{ion}	length of the cube containing one ion in an electrolyte, distance between two ions in the quasi crystals of the Debye-Hückel theory
L	Avogadro-Loschmidt constant
m_{AgI}	amount of AgI
M_{AgI}	molecular mass of AgI
n_0, n_1, n_i	number of primary particles or singlets: at $t=0$, variable of free singlets, of singlets in aggregates of size i
p_i, p_{av}	fraction of singlets: in aggregates of size i, in average aggregates

r, r_a, r_s, r_{sav}, r_{si}	different radii, of aggregates, of stable particles, of average stable particles, of singlets
r_i	reactant fraction of singlets in aggregates of size i
S, S_0, S_ν	Schulze-Hardi rule constant, constant sum of primary particles or singlets in all aggregates, variable sum of the number, ν, of all aggregates
t, t_{crit}, $t_{1/2}$, t_r	time: absolute, critical, half-life or half-period, relative
v, v_s, v_a	titration volume, volume of stable particles, of aggregates
$\pm z$	charge of coagulating counter ions
y_a, y_r, y_s	fraction of singlets in aggregates as products, as reactants, fraction of stable particles
α	collision probability of Smoluchowski's coagulation theory
ΔpAg	$\log[Ag^+] - \log[Ag^+_{\gamma=0}]$
γ, γ_a, γ_e, γ_l	molar quotient = $[I^-_{ads}]/[AgI]$, of aggs, exponential of aggs, linear
$\gamma_e + \gamma_l$, γ_{pept}	molar quotient: $[I^-_{ads}]/[AgI]$: the sum of exponential + linear part, peptized part
Γ^0_e, Γ^0_l	constants of the γ functions: the exponential, the linear
κ	reciprocal Debye-Hückel radius
ν_0, ν_{av}, ν_{avs}, ν_i	number of aggs, at $t=0$, average of aggs., average of stable particles, of aggregates of size i
σ_0	surface charge density
ρ_r, ρ_v, ρ_0	charge density: radial, volume, standard volume
ζ	electro-kinetic potentials, electrophoretic or electro-osmotic
ψ	electrostatic potentials in the vicinity of charges

Acknowledgment. – The author expresses his gratitude to Mr. Zlatko Mihalić, Ph.D., Laboratory of Organic Chemistry and Biochemistry of this Faculty, for his invaluable help in programming and presenting the manuscript and to Mr. Pavel Mildner, Ph.D., Professor (retired), Faculty of Food Technology and Biotechnology, for a critical discussion of the paper.

REFERENCES

1. M. Mirnik, *Croat. Chem. Acta* **65** (1992) 297–307.
2. H. Lichtenfeld, Sonntag and H. Dürr, *Colloids and Surfaces* **54** (1991) 267.
3. M. von Smoluchowski, *Z. Phys. Chem.* **92** (1917) 16.

4. M. Mirnik, *Croat. Chem. Acta* **63** (1990) 113–126.
5. M. Mirnik, Ibid., **61** (1988) 81–101.
6. M. Mirnik, P. Strohal, M. Wrischer, and B. Težak, *Kolloid-Z.* **160** (1958) 146–156.
7. I. A. Valioulis and E. J. List, *Advan. Colloid. Interface Sci.* **20** (1984) 1.
8. I. A. Valioulis, *Advan. Colloid Interface Sci.* **24** (1986) 81.
9. Yu Jiang, *Chem. Phys. Lett.* **224** (1994) 305–307.
10. M. J. Herak, and M. Mirnik, *Kolloid-Z.* **179** (1961) 130–144.
11. D. Tesla-Tokmanovski, M. J. Herak, V. Pravdić, and M. Mirnik, *Croat. Chem. Acta* **37** (1965) 79–90.
12. M. Mirnik, *Croat. Chem. Acta* **42** (1970) 161–214.
13. B. Težak, E. Matijević, and K. Schulz, *Jour. Phys. Chem.* **55** (1951) 1557–1567.
14. E. Matijević, *J. Coll. Interface Sc.* **43** (1973) 217–245.
15. M. Mirnik, and S. Musić, *Progr. Colloid. & Polymer Science* **61** (1976) 36–45.
16. M. Mirnik, *Croat. Chem. Acta* **67** (1994) 493–508.
17. W. Novicki, and G. Novicka, *J. Chem. Educ.* **68** (1991) 523–525.
18. M. Mirnik, *J. Chem. Educ.*, Accepted for publication.
19. J. Lyklema, *Solid Liquid Interfaces*, Academic Press, London, 1987. p 63–90.
20. H. H. Bijsterbosh, and J. Lyklema, *Advances in Colloid Interface Sci.* **9** (1978) 147–251.
21. M. Mirnik, *Croat. Chem. Acta* **64** (1991) 253–268.
22. M. Mirnik, Proceedings, 6th Conference on Colloid Chemistry, Balatonczéplak, 1992, p. 127–131.
23. M. Mirnik, and Collaborators, *Kolloid-Z.*, **163** (1959) 25–31, 32–35, **180** (1962) 51–55, **205** (1965) 111–118, **205** (1965) 120–121, **250** (1972) 950–955, **250** (1972) 956–960; *Croat. Chem. Acta,* **33** (1961) 7–110, **37** (1965) 155–162, **37** (1965) 163–168, **37** (1965) 169–180, **37** (1965) 289–293, **37** (**1965**) 295–302; **38** (1966) 83–90, **43** (1971) 153–167; *Tenside*, **7** (1970) 245–248.
24. M. Mirnik, *Faraday Discussions* **18** (1954) 224–226, 27–28.
25. J. Th. G. Overbeek, in Colloid Science, H. R. Kruyt, Editor, Elsevier, New York, 1952.
26. N. Ise, H. Matsuoka, K. Ito, and H. Yoshida, Faraday Discuss., *Chem. Soc.* **90** (1990) 153.
27. N. Ise, *Croat. Chem. Acta* **68** (1995) 373.
28. M. Mirnik, Ibid. **66** (1993) 509.
29. M. Mirnik, Ibid. **68** (1995) submited for publication.
30. M. Mirnik, Ibid. **50** (1977) 321.
31. M. Mirnik, and B. Težak, Trans. *Faraday Soc.* **50** (1954) 65–72.
32. B. V. Deryagin, L. Landau, *Acty Physcochim. URSS.* **14** (1941) 633–662.
33. E. J. W. Verwey, J. Th. G. Overbeek, *Theory of Stability of Lyophobic Colloids*; Elsevier: New York, 1948.
34. J. Lyklema, *Croat. Chem. Acta* **42** (1970) 151.
35. R. J. Hunter, *Foundations of Colloid Science*, Clarendon Press-Oxford, 1991.
36. S. S. Dukhin, B. V. Derjaguin; Editor, E. Matijević, *Surface and Colloid Science*, 1974, Vol. 7., J. Wiley & Sons, New York, 1974.
37. M. Mirnik, *Faraday Discussions*, **42** (1955) 14, 101, 122, 205, 209, 213, 215.
38. M. Mirnik, F. Flajšman, K. F. Schulz, B. Težak, *J. Phys. Chem.* **60** (1956) 1473–1476.

APPENDIX

[A1]Occasionally, in text books (See *e.g.*, Moore, W. J., Physical Chemistry, Fifth edition, London, 1972, p. 333), Eq. (6) is written as

$$\frac{x}{a \times (a - x)} = k_2 \times t$$

It can be transformed, by multiplying both sides by a, into

$$(x/a)/[(a - x)/a] = a \times k_2 \times t$$

and into the elementary form

$$[\text{product}] \propto p_1 = (1 - r_1) = (1 + 1/t_r) = t_r/(1 + t_r) \tag{6}$$

if one sets $x/a = p_1 = 1 - r_1$ = product fraction, $(a - x)/a = 1 - p_1 = r_1$ = reactant fraction, $a \times k_2 = 1/t_{1/2}$ = reciprocal half-life or half-period, t absolute time, $t_r = t/t_{1/2}$ relative time, a starting concentration of the reactant, x the decomposed or reacted reactant concentration, *i.e.*, the product concentration.

The latter form is instructive because the constant of the second order process is shown to be proportional to the concentration of the reactant, a. This is a characteristic of second order processes. Generally, the constant of the i-th order process is proportional to a^{i-1}.

[A2]Smoluchowski's equation (24)[3] in the original form reads

$$v_\kappa = v_0 \frac{[\alpha v_0 t]^{k-1}}{[1 + \alpha v_0 t]^{k+1}}$$

In the nomenclature of the present paper, it reads

$$v_i = v_0 \frac{[\alpha v_0 t]^{i-1}}{[1 + \alpha v_0 t]^{i+1}}$$

Inserting $\alpha v_0 t = t/t_{1/2} = t_r$ and after division of the nominator and denominator by t_r^{i+1}, one obtains its simpler and elementary form

$$\frac{v_i}{v_0} = t_r^{-2}(1 + t_r^{-1})^{-(i+1)} \tag{10}$$

The corresponding sum (23)[3] reads

$$S_v = \sum_{i=1}^{\infty} v_i/v_0 = \sum_{1+1}^{\infty} t_r^{-2}(1 + t_r^{-1})^{-(i+1)} = 1/(1 + t_r) \tag{11}$$

The same sum is equal to the second order decreasing reactant function (5).

[A3]The (volume) charge density function, ρ_v, of the Debye-Hückel theory reads

$$\rho_v = \frac{\rho_0 e^{-\kappa r}}{(\kappa r)}$$

Multiplied by the relative sphere surface, $4(\kappa r)^2\pi$, one obtains the radial charge density function

$$\rho_r = 4\rho_0 \pi \kappa r e^{-\kappa r}$$

Here, r is the variable distance from the central or reference ion, κ the reciprocal Debye-Hückel radius or distance (See [A3]).

For $r = 1/\kappa$, ρ_r is maximal.

[A4]The well known definition of the reciprocal distance, or radius, κ, of the Debye-Hückel theory reads

$$\kappa^2 = \frac{2e^2 I}{\varepsilon_0 \varepsilon k T}$$

Here, I is the ionic strength of the electrolyte defined by $I = (1/2)\sum c_i z_i^2$. The ionic strength of a binary electrolyte of $z_+ = z_- = 1$ equals its molar concentration. The remaining symbols have the conventional meaning.

[A5]The deduction of Eq. (14):

$$1 \le j \le i_0$$

$$2\sum_{j=1}^{i_0} 2^j = \sum_{j=2}^{i_0} 2^j + 2^{i_0+1}; \quad 2^{i_0+1} = 2\sum_{j=1}^{i_0} 2^j - \sum_{j=2}^{i_0} 2^j;$$

$$(2^{i_0+1} - 2) = 2\sum_{j=1}^{i_0} 2^j - \left(\sum_{j=2}^{i_0} 2^j + 2\right); \quad 2(2^{i_0} - 1) = -2\sum_{j=1}^{i_0} 2^j - \sum_{j=1}^{i_0} 2^j;$$

$$2(2^{i_0} - 1) = \sum_{j=1}^{i_0} 2^j;$$

$$S_0 = 2\sum_{j=1}^{i_0} j \times v_j = 2i_0\sum_{j=1}^{i_0} 2^j = 4i_0(2^{i_0} - 1) = i_{av} \times v_{av} \qquad (14)$$

Example: $i_{av} = i_0 = 6$; $v_{av}(i_{av} = i_0 = 6) = 252$; $S_0 = 1512$

[A6] *E.g.*, Derjaguin, Landau, Verwey, Overbeek (*DLVO*)[32, 33] theory predicts the following formulation of the Schulze-Hardy rule

$$[M^z]/[M^1] = |z|^{-6}$$

The same rule has never been confirmed experimentally.

Lyklema, J.[34] tried to explain the divergence between the sixth power formulation of the Schulze-Hardi rule of the *DLVO* theory and the experimentally many times confirmed linear formulation (18) by claiming, that the high surface potential is usually not encountered in practice. He assumed, namely, that the surface potential equals the Nernst potential. Consequently, it can be assumed that it is proportional to ΔpAg. All, high and low potentials are normally encountered, i.e., $10 \approx< \Delta pAg >\approx -4$ or $1 \approx< pI <\approx 15$ values. The Nernst potential can be measured as the electromotive force, EMF, between the poles of an electrometer connected with metallic wires to two metallic electrodes in Galvanic cells. The latter have at least three phases. Colloidal systems (*e.g.*, AgI/electrolyte) have only two phases and no metallic phase. The charging of a metallic electrode is a process of oxidation and reduction of «potential determining« ions while the process of charging a coloidal particle is ion adsorption. This is a sufficient proof that the Nernst potential can neither arise on colloidal particles nor have any physical significance in colloids.

Immersion of the cell »*Ag|AgI. electrolyte|standard electrode*« in the sol for potentiometric determination of pI or pAg does not affect the double layer on sol particles.

J. Lyklema,[34] expressed the opinion that comparisons of experimental results with predictions of the DLVO theory must be rejected for historical reasons (*Ibid.*, p. 153). Non existing surface potentials and historical reasons are certainly no arguments for any criticism of any theory. The only method of checking the usefulness and correctness of a theory has always been and will always be its comparison with experiments.

[A7] Ise claims[27] that $2D_{exp}$ is not a projection but a real inter particle distance. Figure 15. and its description is an axiomatic proof that the claim is erroneous.

SAŽETAK

Teorije koloidne kemije temeljene na modelu točkastih naboja dvosloja

Mirko Mirnik

Na temelju eksperimentalnih i teorijskih razmatranja pokazano je da je koagulacija reakcija 2. reda kojom nastaju agregati veličine šest primarnih čestica. Grafički je pokazano da se teorijske funkcije dobro poklapaju s teorijskima. Opisani su nedostaci teorije koagulacije Smoluchowskoga. Dokazano je, da se tom teorijom ne